Electrical-resistivity imaging of the central Trans-Hudson orogen[1, 2]

Ian J. Ferguson, Kevin M. Stevens, and Alan G. Jones

Abstract: Magnetotelluric (MT) measurements were made on a profile across the Trans-Hudson orogen in 1992 as part of the Lithoprobe transect. The present study includes analysis of results from a 300 km-long section of the profile in which allocthonous Paleoproterozoic juvenile terranes and arc rocks of the western Trans-Hudson orogen have been juxtaposed against the Archean Sask craton. Impedance tensor decomposition of data from the 40 MT sites in the area indicates a geoelectric strike of N28°E. Two-dimensional inversion of the data using a non-linear conjugate gradient algorithm provided images of the resistivity structure. Resistivity images reveal that the crust of the Sask craton is relatively resistive (>2000 Ω·m). In contrast, the rocks of the Flin Flon belt, Glennie domain, and La Ronge domain are mostly relatively conductive (<100–1000 Ω·m). In the east of the study area, the images suggest that the Tabbernor fault juxtaposes more conductive rocks of the Glennie domain in the west against more resistive Archean rocks in the east in the upper 20 km of the crust. In the west of the study area, the images confirm that the North American Central Plains conductor occurs within westward-dipping rocks of the La Ronge domain. The resistivity images also reveal that the lower crust beneath the west of the Glennie domain, within a crustal culmination defined by seismic reflection data, is electrically conductive (<100 Ω·m). An explanation for the enhanced conductivity is that part of the lower crust beneath the western Glennie domain is of Proterozoic age. In this case, a possible source for the enhanced conductivity, based on its location at the edge of the Sask continental block, is Proterozoic ocean margin rocks.

Résumé : Des mesures magnétotelluriques (MT) ont été effectuées sur un profil à travers l'orogène trans-hudsonien en 1992 dans le cadre du transect lithoprobe. La présente étude comprend l'analyse des résultats d'une section de 300 km de long du profil dans lequel des terranes juvéniles allochtones (Paléoprotérozoïque) et des roches d'arc de l'orogène trans-hudsonien occidental ont été juxtaposés contre le craton Sask (Archéen). La décomposition du tenseur d'impédance des données des 40 sites MT dans la région indique une direction géoélectrique de N28ºE. Une inversion bidimensionnelle des données au moyen d'un algorithme conjugué, non linéaire, du gradient a fourni des images de la structure de résistivité. Les images de résistivité révèlent que la croûte du craton Sask est relativement résistive (>2000 Ω·m). Par contraste, les roches de la ceinture de Flin Flon, du domaine de Glennie et du domaine de La Ronge sont surtout relativement conductrices (<100–1000 Ω·m). Dans la partie est de la région à l'étude, les images suggèrent que la faille Tabbernor juxtapose des roches plus conductrices du domaine de Glennie à l'ouest contre des roches archéennes plus résistives à l'est dans les 20 km supérieurs de la croûte. Dans la partie ouest de la région à l'étude, les images confirment que le conducteur des plaines centrales de l'Amérique du Nord se trouve à l'intérieur des roches à pendage vers l'ouest du domaine de La Ronge. Les images de résistivité révèlent aussi que la croûte inférieure sous la partie ouest du domaine de Glennie, à l'intérieur d'une culmination de la croûte définie par des données de sismique réflexion, a une conductivité électrique (<100 Ω·m). Une explication pour la conductivité rehaussée est qu'une partie de la croûte inférieure sous le domaine de Glennie occidental est d'âge protérozoïque. Dans ce cas, une source possible pour la conductivité rehaussée, basée sur sa localisation à la bordure du bloc continental Sask, serait les roches protérozoïques de la marge océanique.

[Traduit par la Rédaction]

Introduction

The Trans-Hudson orogen (THO) is a Paleoproterozoic orogenic belt forming part of a major North American system extending from South Dakota, across Hudson Bay, into Labrador and Greenland (Lewry and Collerson 1990). It has been divided into four constituents: (1) the internal part of the orogen, the Reindeer Zone, contains juvenile arc related

Received 12 November 2003. Accepted 20 January 2005. Published on the NRC Research Press Web site at http://cjes.nrc.ca on 17 June 2005.

Paper handled by Associate Editor F. Cook.

I.J. Ferguson.[3] Dept. of Geological Sciences, University of Manitoba, Winnipeg, MB R3T 2N2, Canada.
K.M. Stevens. Falconbridge Exploration Limited, PO Box 40, Falconbridge, ON POM 1SO, Canada.
A.G. Jones.[4] Geological Survey of Canada, 615 Booth Street, Ottawa, ON, K1A 0E9, Canada.

[1]This article is one of a selection of papers published in this Special Issue on *The Trans-Hudson Orogen Transect of Lithoprobe*.
[2]Lithoprobe Publication 1396.
[3]Corresponding author (e-mail: ij_ferguson@umanitoba.ca).
[4]Present address: Dublin Institute of Advanced Studies, 5 Merrion Square, Dublin 2, Ireland.

 doi: 10.1139/E05-017

Fig. 1. Major geological divisions of the Trans-Hudson orogen (modified from Lucas et al. 1994). WD, Wollaston domain; WB, Wathaman batholith; RD, Rottenstone domain; LRD, La Ronge domain; GD, Glennie domain; HLB, Hanson Lake block; KD, Kisseynew domain (Kisseynew Gneiss Belt); FFB, Flin Flon belt; SBZ, Superior boundary zone; TF, Tabbernor fault; W, window of exposed Archean rock. The box shows the area of the present study.

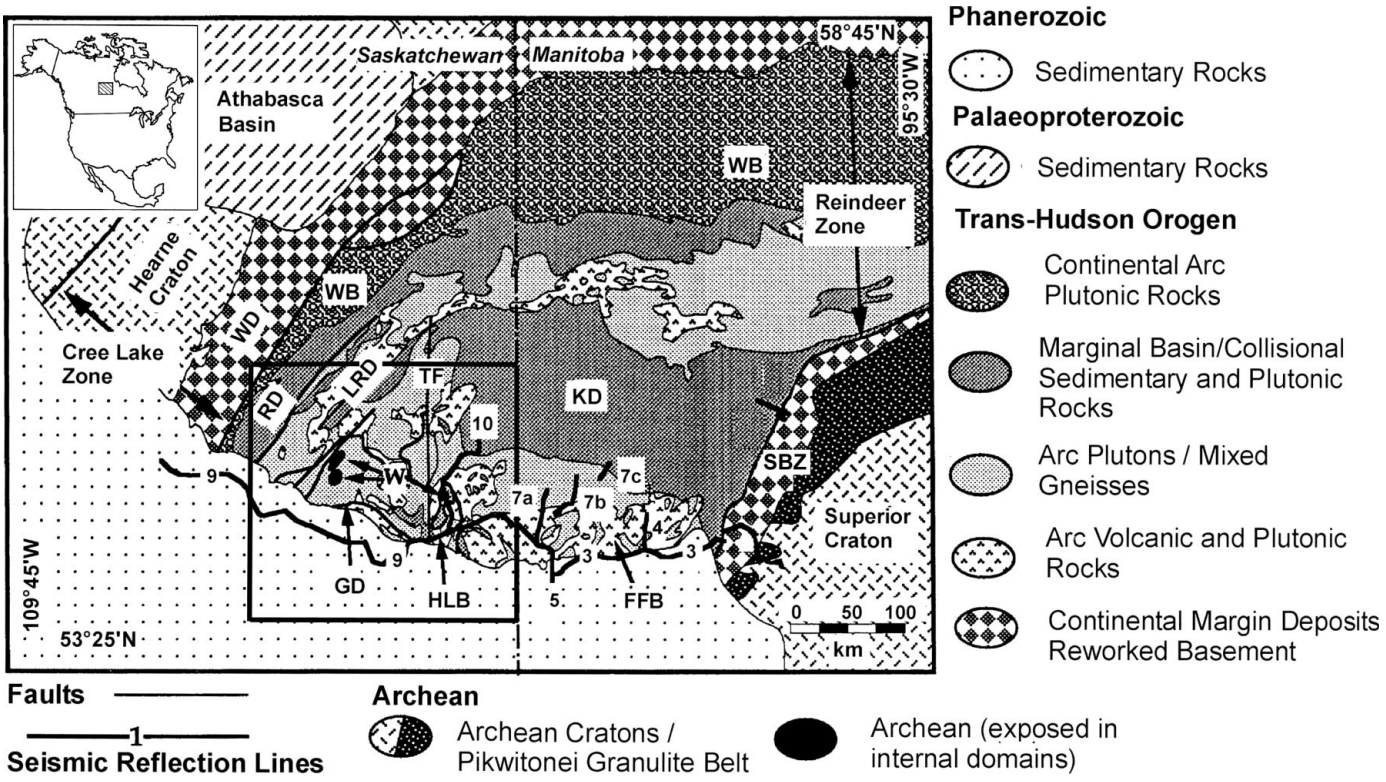

volcanic and plutonic rocks and adjacent sedimentary basin rocks; (2) the Wathaman batholith is an Andean type mainly granitic plutonic complex; (3) the Superior boundary zone is a narrow zone of reworked cratonic rocks forming the eastern margin of the orogen; and (4) a complexly deformed hinterland including the Wollaston domain forming the north and northwestern margin between the THO and the Rae–Hearne Province (Fig. 1). Locally exposed Archean rocks within the central Reindeer zone are interpreted to represent part of the buried Sask craton. The objective of the Lithoprobe studies of the THO was to determine the crustal structure and characteristics of the internal components and margins of the orogen to understand the tectonic development of the collisional zone (Clowes 1989).

In this study, the magnetotelluric (MT) method is used to image the electrical resistivity structure of the central THO in Eastern Saskatchewan and western Manitoba, Canada. In Precambrian crustal rocks the primary sources of enhanced electrical conductivity in the upper crust are graphite, metallic sulphides, metallic oxides and possibly less conducting minerals, such as serpentinite (e.g., Jones 1992). Aqueous fluids present in shear zones or trapped within the crust may also contribute to the conductivity. Electrical resistivity images delineate geological units containing different proportions of these components. For example, metasedimentary rocks containing graphite can be significantly conductive. The electrical resistivity is usually much more sensitive to these mineral constituents than are other physical properties including density, seismic velocity, and acoustic impedance, and as a result electromagnetic (EM) methods can often provide better resolution of geological units containing these constituents.

The MT method is based on the principle that EM signals with different periods penetrate to different depths into the earth: thus surface measurements of the EM response can determine the resistivity at a range of depths (Vozoff 1991). Short-period MT signals (10^{-4} to 10^{-3} s) penetrate 2–10 km into the upper crust, whereas long-period signals (10^{3}–10^{4} s) penetrate 100 km or more, into the upper mantle. In the present study, the MT method is used to image the resistivity structure of the THO and overlying Phanerozoic sedimentary rocks at depths ranging from several tens of metres to ~100 km.

The specific aim of the Lithoprobe MT surveys in the THO was to resolve the form of the resistivity structure of the lithological domains forming the orogen and of major faults and shear zones. An important objective of both the overall Lithoprobe studies and the MT work was to establish the spatial and structural relationships of the North American Central Plains (NACP) conductivity anomaly, a major 2000 km-long electrical conductivity anomaly lying within the THO. The present study describes an investigation of the central part of the Reindeer Zone. The sites considered in this study cross a number of internal units of the Reindeer Zone: the Flin Flon belt, Hanson Lake block, Glennie domain, La Ronge domain and Rottenstone domain as well as a number of faults and shear zones including the Sturgeon–Weir shear zone, Tabbernor fault, and Stanley fault. This profile defined by the MT sites is of particular interest since it crosses the interpreted position of the buried Archean Sask craton, and

Fig. 2. Major geological structures in the study area (after Lewry et al. 1994; Hajnal et al. 1996). SWSZ, Sturgeon–Weir shear zone; HSZ, Hartley shear zone; SF, Stanley fault; GCT, Guncoat thrust; BRSZ, Birch Rapid "straight belt"; TF, Tabbernor fault; SW, Sahli window; MW, MacMillan Point window; HW, Hunter Bay window; NW, Nistowiak–Iskwatikan window.

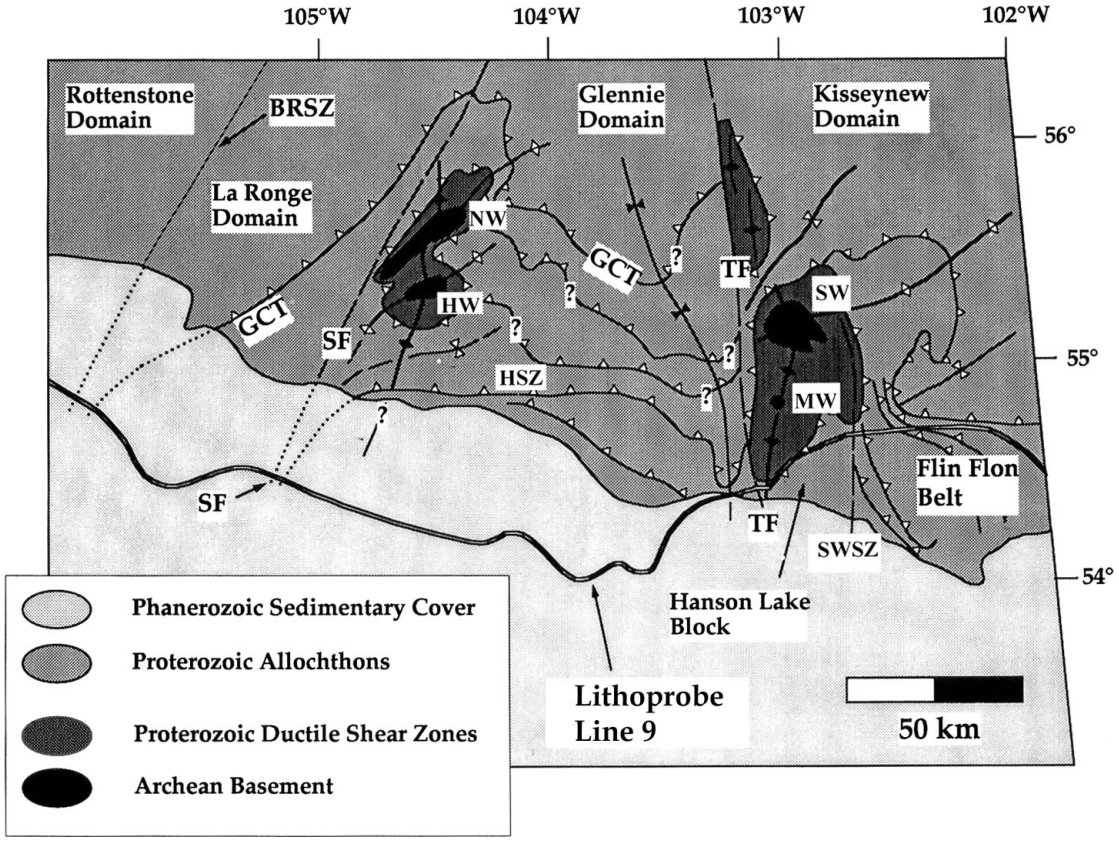

the MT data will enable the imaging of the resistivity structure of the craton. Finally, the westernmost sites in the present study cross the NACP conductor and allow detailed examination of the tectonic setting of the conductor. The paper by Jones et al. (2005) in this volume considers the NACP conductor in greater detail.

Regional geology

Geological units

The Reindeer Zone is a 400 km-wide collage of Paleoproterozoic arc volcanic and plutonic rocks, coeval and derived volcanogenic sediments, arkosic molasse, and late post-kinematic intrusions. Archean rocks exposed in, and present beneath, the central Reindeer Zone are interpreted to represent part of a buried craton known as the Sask Craton in Canada (Ansdell et al. 1995). The Archean rocks occur in tectonic windows produced by late cross-folding. In the Hanson Lake block the Archean rocks occur in the Sahli and MacMillan Point windows (Lewry et al. 1994) (collectively referred to as the Pelican window) and in the western Glennie domain the Archean rocks occur in the Nistowiak Lake – Iskwatikan Lake and Hunter Bay windows (Fig 2). The Archean basement is everywhere separated from Proterozoic allochthons by mylonitic gneisses (Chiarenzelli et al. 1996). This geometry and the wide occurrence of reworked Archean crust and its plutonic derivatives in sub-Phanerozoic drill-core farther south suggest that Archean rocks may underlie much or all of the Reindeer Zone (Lewry et al. 1994).

The Flin Flon belt is a low-grade metavolcanic–plutonic belt. The central part of the belt consists of a collage of intra-oceanic assemblages formed in a range of tectonic environments. These 1.92–1.88 Ga assemblages were tectonically juxtaposed into an accretionary complex, the Amisk Collage, at 1.88–1.87 Ga (Lucas et al. 1996). The Kisseynew domain (or gneiss belt), which bounds the Flin Flon belt to the north is dominated by migmatitic, amphibolite-grade, turbiditic, greywackes deposited in a back-arc setting adjacent to the Flin Flon arc at ca. 1.85–1.84 Ga (Ansdell et al. 1995; David et al. 1996). The Hanson Lake block and Glennie domain are dominated by granitoid rocks with subordinate to minor supracrustal rocks. The Hanson Lake block contains volcano-plutonic and intrusive rocks, correlative with the Flin Flon belt (Ashton and Lewry 1994, 1996; Ashton et al. 1999). It has been proposed that the Glennie domain, Hanson Lake block, and possibly the Flin Flon belt represent a single arc complex (Ashton et al. 1997; Maxeiner et al. 1999).

Within the study area the La Ronge arc comprises 1.91–1.88 Ga mafic volcanic rocks, intermediate to felsic arc volcanics, ocean-floor and back-arc volcanics and turbiditic sedimentary rocks deposited between 1.92 and 1.86 Ga (Yeo et al. 2001). The eastern La Ronge domain is dominated by high-grade metasedimentary migmatites (Lewry et al. 1994). The western La Ronge domain consists mainly of low metamorphic grade mafic to felsic metavolcanic rocks and

granitoid plutons (Lewry et al. 1994). The Rottenstone domain contains a tonalite–migmatite belt and the calc-alkaline affinity Wathaman batholith, dated at ca. 1.85, which is interpreted as the root of Andean-type continental arc (Lewry et al. 1994). The Wathaman batholith is separated from the Archean Hearne Province by the Cree Lake Zone of the Wollaston domain. This zone is dominated by amphibolite- to granulite-facies granitoid orthogniesses, migmatites, and minor mafic gneisses. It is interpreted to record an evolution from a rifted continental margin to a foreland fold–thrust belt as outboard terranes collided with the Hearne cratonic margin.

The MT profile in the present study includes some sites located on gently dipping Phanerozoic sedimentary rocks to the south of the Precambrian shield. These rocks form part of the Williston basin. In the east of the study area, the Phanerozoic rocks form part of the Ordovician Red River and Winnipeg formations, and in the east of the study area, the rocks form part of the Cretaceous Mannville group and Lower Colorado group (MacDonald and Broughton 1980).

Tectonic history and structural features

Lucas et al. (1997) describe the tectonic evolution of the Reindeer Zone. This process involved the closure, during the Paleoproterozoic, of the 5000-km wide Manikewan ocean (Symons et al. 1995). Deformation was driven by the convergence of the Archean Superior and Rae–Hearne cratons and northwest movement of the Sask craton within the narrowing ocean. The present geometry of the central Reindeer Zone reflects the initial deformation that occurred during accretion between 1.88 and 1.87 Ga. The La Ronge arc formed towards the western margin of the ocean between 1.92 and 1.86 Ga, predating the Wathaman magmatism which occurred ca. 1.85 Ga. Extensive deformation was associated with terminal collision between the Reindeer Zone and Superior craton, including south to southwest translation of Reindeer Zone allochthons over the Archean footwall basement of the Sask craton between 1.83 and 1.79 Ga (Lewry et al. 1994). The main tectonism involved fold–thrust stacking and the transportation of major allocthonous sheets, some of which are soled by regionally extensive high strain zones (Lewry et al. 1990).

In the allochthonous thrust sheet classification of Lewry et al. (1990), the Cartier sheet, which consists mainly of Glennie domain rocks, overlies Archean basement rocks. In the Hanson Lake block, the Pelican thrust forms a major detachment zone marking the contact between the Proterozoic rocks and the Archean rocks in the Pelican window. In the western Glennie domain, the Nistowiak and Hunter Bay windows are also separated from Proterozoic rocks by similar mylonites (Chiarenzelli et al. 1996). It is speculated that these mylonitic gneisses accommodated the subhorizontal translation of arc rocks over the Sask craton during initial convergence (Lewry et al. 1990).

The Cartier sheet is overlain by the Wapassini sheet, which is composed mainly of southeast La Ronge domain rocks. The Wapassini sheet is soled by tectonic schists and mylonitic gneisses of Guncoat gneisses, the upper unit of which is defined as the Guncoat thrust (Fig. 2). Baird and Clowes (1996) suggest that the seismic signature of the Guncoat thrust has a width of around 20 km where it crosses the Lithoprobe transect. Hajnal et al. (1996) show the Hartley Shear zone to be a shallow west-dipping structure parallel to the Guncoat thrust and defining the boundary between the Glennie and La Ronge domains. According to the thrust sheet classification of Lewry et al. (1990), the Hartley shear zone would represent an internal structure in the Cartier sheet. Along the southern margin of the shield, near the Lithoprobe transect, the Wapassini sheet appears to extend to the western margin of the Rottenstone domain. This belt is lithologically transitional into the lower grade rocks of the La Ronge domain, but in the study area, the junction is defined by the eastern boundary of the Birch Rapids straight belt, a zone of ductile high strain and later brittle cataclasis (Lewry et al. 1990; Schwerdtner and Cote 2001). North of the study area the Wapassini sheet is overlain by the Kyaska sheet of Lewry et al. (1990), which includes mainly rocks of the Kisseynew domain but also rocks of the MacLean Lake belt of the La Ronge domain.

The Sturgeon–Weir shear zone separates the Hanson Lake block from the Flin Flon belt. In earlier interpretations, the shear zone was interpreted to be a major, steeply dipping, crustal-scale structural boundary. On the basis of the reprocessing of seismic reflection data by Pandit et al. (1998), it is interpreted to dip at a shallow angle to the east. Ashton and Lewry (1996) suggest the shear involved a relatively small displacement within an already amalgamated protocontinent.

There are several major orogen-parallel high-angle faults in the study area associated with the post-collisional intracontinental deformation. Some of these faults were active during earlier collisional deformation and initial folding of the basement and cover in the Reindeer Zone. It is speculated that the post-collisional activation of the faults was kinematically linked to low-angle ductile shearing in the mid to lower crust (Hajnal et al. 1996). The deformation produced orogen-parallel extrusion of the internal units relative to the bounding Archean cratons. The Needle Falls shear zone is a high-angle fault, which at the surface defines the margin of the Wathaman batholith with the Wollaston domain. The Tabbernor fault forms the margin of the Hanson Lake block with the Glennie domain (Fig. 2) (Elliot 1996). It underwent sinistral oblique ductile shear in the early Proterozoic followed by sinistral strike slip motion along discrete brittle faults. There has been significant debate as to the tectonic significance of the Tabbernor fault. Although, it can be traced for more than 1500 km along strike and there is evidence of its re-activation during Phanerozoic and recent time, to the north of the study area, there is only small offset of tectonic units across the fault (Lewry et al. 1990; Elliot 1996). The brittle–ductile Stanley fault occurs near the boundary between the La Ronge domain and the Glennie domain at the latitude of the Lithoprobe THO profile (Baird and Clowes 1996). As with the Tabbernor fault, the significance of this fault to the regional structure is now believed to be less than once proposed (Lewry et al. 1990).

Previous magnetotelluric and electromagnetic studies

A number of previous MT and geomagnetic depth sounding studies have been completed in the THO in Canada. The

Fig. 3. Location of MT sites used in this study. The study area covers approximately the area shown in Fig. 2. NFSZ, Needle Falls shear zone; A*xx*, AMT site; M*xx*, BBMT site; L*xx*, LMT site. See Figs. 1 and 2 for other abbreviations.

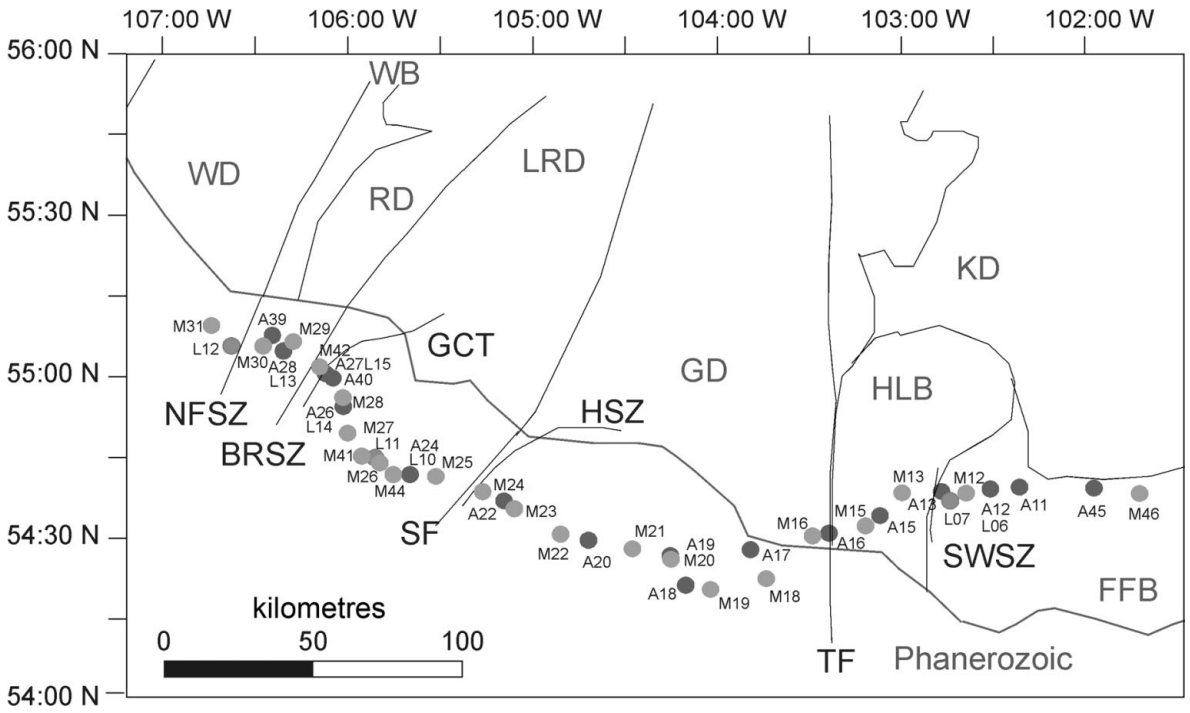

NACP conductivity anomaly has been the focus of these studies (see review by Jones et al. 2005, this issue). Within Canada the NACP anomaly runs north through Saskatchewan beneath the Phanerozoic Williston basin. North of the present survey location it turns east and follows the rocks of the THO beneath Hudson Bay. In more recent studies done as part of the Lithoprobe project, Jones et al. (1993, 1997*a*) have analysed data from the Glennie domain, La Ronge domain, and Rottenstone domain to image the conductor. Additional petrophysical studies have suggested that the cause of the enhanced conductivity is the presence of sulphides that have been anisotropically concentrated in fold hinges (Katsube et al. 1996; Jones et al. 1997*a*).

A number of other MT studies have been completed within the Lithoprobe THO project. Jones and Corriea (1992) describe results from a preliminary survey in eastern Saskatchewan overlapping with the present survey area. Jones and Kalvey (1993) describe MT soundings in the western margin of the THO. Grant (1997*a*, 1997*b*) and Jones et al. (1997*b*) describe preliminary integrated results from across the transect. Ferguson et al. (1999) examined the response in the Flin Flon belt to the east of the present study area. White et al. (1999, 2000) have examined the resistivity structure of the eastern margin of the orogen. To create a continuous resistivity model across the THO, the profile in the present study overlaps at its margins with those of the studies of Jones et al. (1993) and Ferguson et al. (1999).

Lithoprobe 1992 THO magnetotelluric survey

The Lithoprobe 1992 THO MT survey involved data collection at audio-frequency MT (AMT) sites which provided the response for the period range 10^{-4} to 10^{-1} s, and broad-band MT (BBMT) sites which provided the response for the period range 10^{-4} to 1820 s. AMT sites were located between adjacent BBMT sites to provide additional information on the upper crustal conductivity structure. The complete survey included a total 56 BBMT sites and 52 AMT sites located along an 800-km profile with an average spacing between BBMT sites of 15 km and an average spacing between BBMT and AMT sites of 7 km. Where access permitted, the MT sites were located on the Phanerozoic sedimentary rocks to the south of the exposed shield in an attempt to reduce distortion of the MT response by near-surface heterogeneities in the resistivity structure. Data acquisition at the BBMT and AMT sites was undertaken between June and September 1992 by commercial contract to Phoenix Geophysics. Additional long-period MT (LMT) soundings using LiMS (long-period magnetometer system) instruments (Andersen et al. 1988) belonging to the Geological Survey of Canada were also completed with sites at selected locations in the orogen. Details of the field procedures for the AMT, BBMT, and LMT sites are provided in Ferguson et al. (1999).

The present study involves the analysis of data from 24 BBMT (M*xx*), 18 AMT (A*xx*), and eight LMT (L*xx*) sites located on a 200 km-long section of the profile in eastern Saskatchewan (Fig. 3). Phoenix Geophysics provided the BBMT and AMT responses for each site in the form of auto- and cross-power spectra, computed using robust statistical techniques based on the Jones–Jödicke approach (Jones and Jödicke 1984; method 6 in Jones et al. 1989). Time series collected in the long-period MT survey were analyzed using the same robust processing procedures. Data segments were merged and analyzed using remote-reference processing. The processing employed robust spectral analysis and jack-knife error estimation (Jones and Jödicke 1984). The responses from several of the MT sites were excluded from parts of the

Fig. 4. Swift skew response in the study area. Crosses show data points. Skew values above about 0.25–0.3 indicate significantly 3-D structures or 3-D distortion. Tectonic boundaries are shown in the same locations as in Fig. 2. NFSZ, Needle Falls shear zone; see Figs. 1 and 2 for other abbreviations.

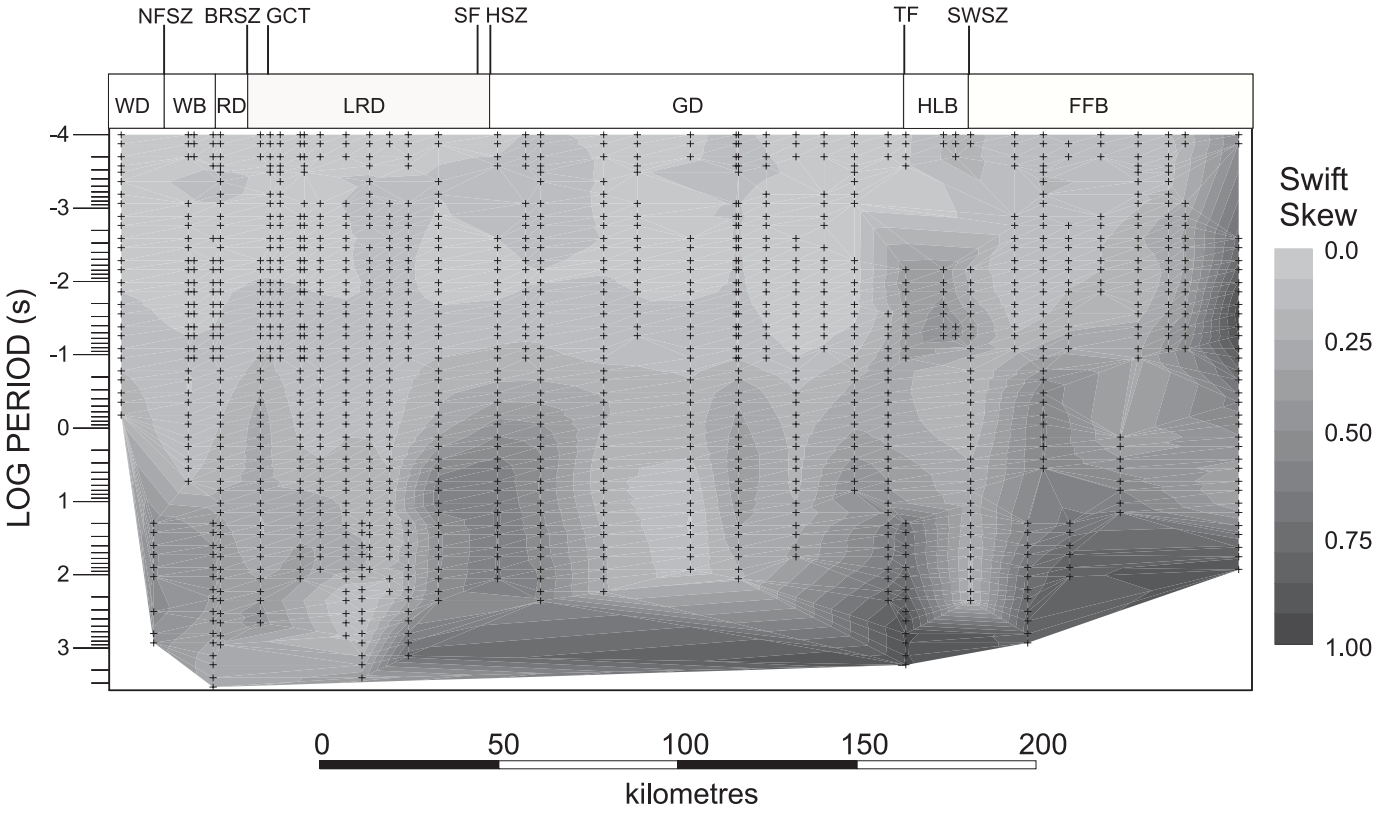

analysis in this study because of the presence of band-limited noise at MT sites located within several kilometres of railways and mining camps and severe distortion due to near-surface heterogeneities at a number of LMT sites.

Geoelectric dimensionality, distortion, and strike azimuth

The primary response obtained at each MT site is a tensor containing the complex-valued frequency-dependent transfer functions or impedances relating the measured horizontal electric and horizontal magnetic field components. The magnitudes of the off-diagonal impedance tensor elements can be transformed to equivalent apparent resistivity values, which in the case of one-dimensional (1-D) structures represent averaged resistivity over the penetration depth of the signals (Vozoff 1991). The phase of the impedance terms also contains information on the resistivity structures. The EM fields over a 2-D structure, in which the resistivity structure is invariant in the geoelectric strike direction, can be divided into two independent modes. These modes involve electric current flow parallel to strike, the transverse electric or TE mode, and electric flow perpendicular to strike, the transverse magnetic or TM mode. The corresponding MT impedances provide complementary information on the 2-D resistivity structure.

A second response obtained in MT surveys is the magnetic transfer function (or tipper) response, which relates the vertical component of the magnetic field to the two horizontal components (Vozoff 1991). This response is often displayed graphical in the form of induction arrows. The direction of the reserved real component of the induction arrow will be orthogonal to the local geoelectric strike, and for simple 2-D structures, the arrow will point towards more conductive regions (Parkinson 1962; Jones 1986).

Dimensionality

An important first step in the analysis of MT data is to examine whether the impedance response at each site is consistent with a 1-D or 2-D structure or whether it indicates a structure with a more complex 3-D form. The Swift skew provides a measure of the departure of the response from either a 1-D or 2-D form. It typically exceeds 0.25–0.3 in significantly 3-D structures (Vozoff 1991), but for sites with appropriate symmetry relative to the structure, it can have lower values (Groom and Bailey 1989). Figure 4 shows the skew determined for the present study area. In general, the skew increases with increasing period as the response becomes sensitive to regions at greater depth and distance from the site. At most sites, the skew is < 0.3 at periods < 100 s, consistent with the crustal structures being close to 1-D or 2-D in form. Overall the results suggest that if the modelling is restricted to the data in the period range 10^{-4} to 100 s, then a 2-D modelling approach will be reasonably valid. Appropriate care should be taken in the interpretation of results derived from more regions with stronger 3-D responses.

There are three locations in the study area in which larger

skew is noted. At sites in the Flin Flon belt, the skew becomes progressively larger at specific periods with distance to the east. This response is likely because of the increasing proximity to east–west-striking features, such as the contact of the Flin Flon belt and the Kisseynew domain. Relatively high skew is noted at short periods (~10^{-2}–10^{-1} s) at sites on or adjacent to the Hanson Lake block suggesting 3-D structures at crustal depth in this area. Jones and Correia (1992) report a similar result. Interpretation of seismic reflection data from lines parallel to the MT profile (line 9) and perpendicular to it (line 10), e.g., Pandit et al. (1998), confirms the presence of such 3-D structures. Finally, relatively high skew is noted at intermediate periods (>1 s) at sites on the margin of the Glennie domain.

Distortion

A special class of 3-D resistivity structures is one in which the regional response has a 1-D or 2-D form, but the observed response is distorted by near-surface heterogeneities. If the coordinate system of the data is orthogonal to the regional geoelectric strike, the distortion is characterized by a frequency-independent shift of the impedance magnitude and the corresponding apparent resistivity response called static shift. In more complex geometries, the distortion will result in mixing of the impedance terms. However, as long as the regional geoelectric strike is correctly identified, and the responses are rotated into a coordinate system orthogonal to the regional strike, the phases will not be affected by the distortion.

The distortion of the MT data from eastern Saskatchewan was examined using the Groom–Bailey (GB) tensor decomposition method (Groom and Bailey 1989, 1991; Groom et al. 1993), in which a parameterization of the near-surface distortion effects is done simultaneously with a determination of the regional geoelectric strike. In the GB method, the phase-related galvanic distortion at each frequency is characterized by two parameters: *shear*, which provides a measure of the local polarization of the electric field response, and *twist*, which provides a measure of its local rotation. A number of conclusions can be drawn from the distortion responses (Stevens 1998). Firstly, the average distortion was larger for sites on the exposed Precambrian shield than for sites on the Phanerozoic sedimentary rocks. Secondly, the responses are inconsistent with a physical model in which the distortion is caused by only near-surface features. In this case, the shear and twist would be independent of period. For the present MT data, a gradual increase in shear and twist occurs over intermediate to long periods, suggesting the presence of heterogeneities at a variety of spatial scales in the crust. Finally, the irregularities in the final regional strike angles suggest that the distortion model is not well defined statistically at individual periods and individual sites.

Regional strike azimuth

To define the regional strike more consistently, Grant (1997*a*) used multi-frequency GB decompositions, in which the regional strike and distortion are constrained to be constant over a specified period range. He considered the full period range from 10^{-4} to 10^{3} s for the BBMT sites and the period range from 10^{-4} to 10^{-1} s for AMT sites. The results are shown in Fig. 5 and indicate strikes varying from 12°–23° in the Rottenstone–Wathaman–Wollaston part of the transect, 12°–37° in the La Ronge domain, and 32°–45° in the Glennie domain. The distortion is too high, the GB fit is too poor, or the noise level is too high to allow effective single-site determinations at the BBMT sites in the Hanson Lake block and Flin Flon belt. This observation is in agreement with the high skew noted in these areas in Fig. 3. Grant (1997*a*) also did multi-site multi-frequency GB decompositions using the method of McNeice and Jones (2001), in which the data from a number of sites are fitted by a model in which the regional strike is constant at all sites. These analyses indicate a geoelectric strike of around N30°E.

The combined geoelectric strike results from Grant (1997*a*), Stevens (1998), and from GB analyses of the LMT data, for a total of 42 MT sites, have a mean azimuth of N28°E with a standard deviation of 12°. Because of the varying approaches used in the determinations, the standard deviation is not a statistically valid estimate for the true variability in the strike azimuth. However, when it is considered in combination with the skew results, the standard deviation suggests that 2-D modelling with a strike azimuth of N28°E is a reasonable approach to the determination of the crustal resistivity structure. In further examination and modelling, the data are rotated so that the TE response corresponds to electric currents flowing at N28°E azimuth and the TM responses corresponds to currents flowing at N118°E azimuth.

Induction vectors

Figure 5 shows the real induction arrows for a 30 s period. This response is typical of the longer period induction arrows. At shorter period, the responses are more erratic. The 30 s induction arrow responses in the west of the study area are dominated by arrows pointing west towards a location in the central western La Ronge domain. Jones et al. (1993) showed that this is the location of the NACP conductor and that the induction arrows are responding to this structure. The induction vectors in the east of the study area are more erratic than those in the west. At a number of sites the arrows have a significant northward component and point towards the Kisseynew domain. This response, which was also noted in Ferguson et al. (1999), suggests the presence of an east–west-striking boundary in conductivity between the Flin Flon belt and enhanced conductivity in the Kisseynew domain. Such a 3-D resistivity structure would contribute to the high values of skew noted in this part of the profile.

Magnetotelluric responses

Figure 6 shows pseudosections of the MT apparent resistivity and phase response for the TE and TM modes. The horizontal axis corresponds to the location on the line perpendicular to strike and increasing period down the page corresponds to increasing depth of signal penetration. The phase response is related to the gradient of resistivity. Phase values close to 45° indicate that the resistivity is relatively uniform with depth, values exceeding 45° indicate an increase in conductivity with depth, and values < 45° indicate an increase in resistivity with depth. Differences between the TE and TM responses provide an indication of the presence of significantly 2-D structures.

To the west of the Tabbernor fault, the MT responses define a near-surface conductor that deepens to a maximum at a

Fig. 5. Geoelectric strikes determined for the study area. (*a*) Strike directions determined by Grant (1997*a*) using single-site multi-frequency GB decompositions. The strike was determined using the period range from 10^{-4} to 10^{3} s for BBMT sites and 10^{-4} to 10^{-1} s for AMT sites. Sites at which the strike direction could not be adequately resolved are indicated by the absence of a strike direction symbol. (*b*) Real component of induction arrows for 30 s period. Arrows are plotted with the Parkinson (1962) convention and point toward conductive regions. Sites for which the induction arrow is not well resolved have been omitted. Induction arrow scale: a distance of 75 km on the distance scale bar corresponds to an arrow magnitude of 1.0. NFSZ, Needle Falls shear zone; see Figs. 1 and 2 for other abbreviations.

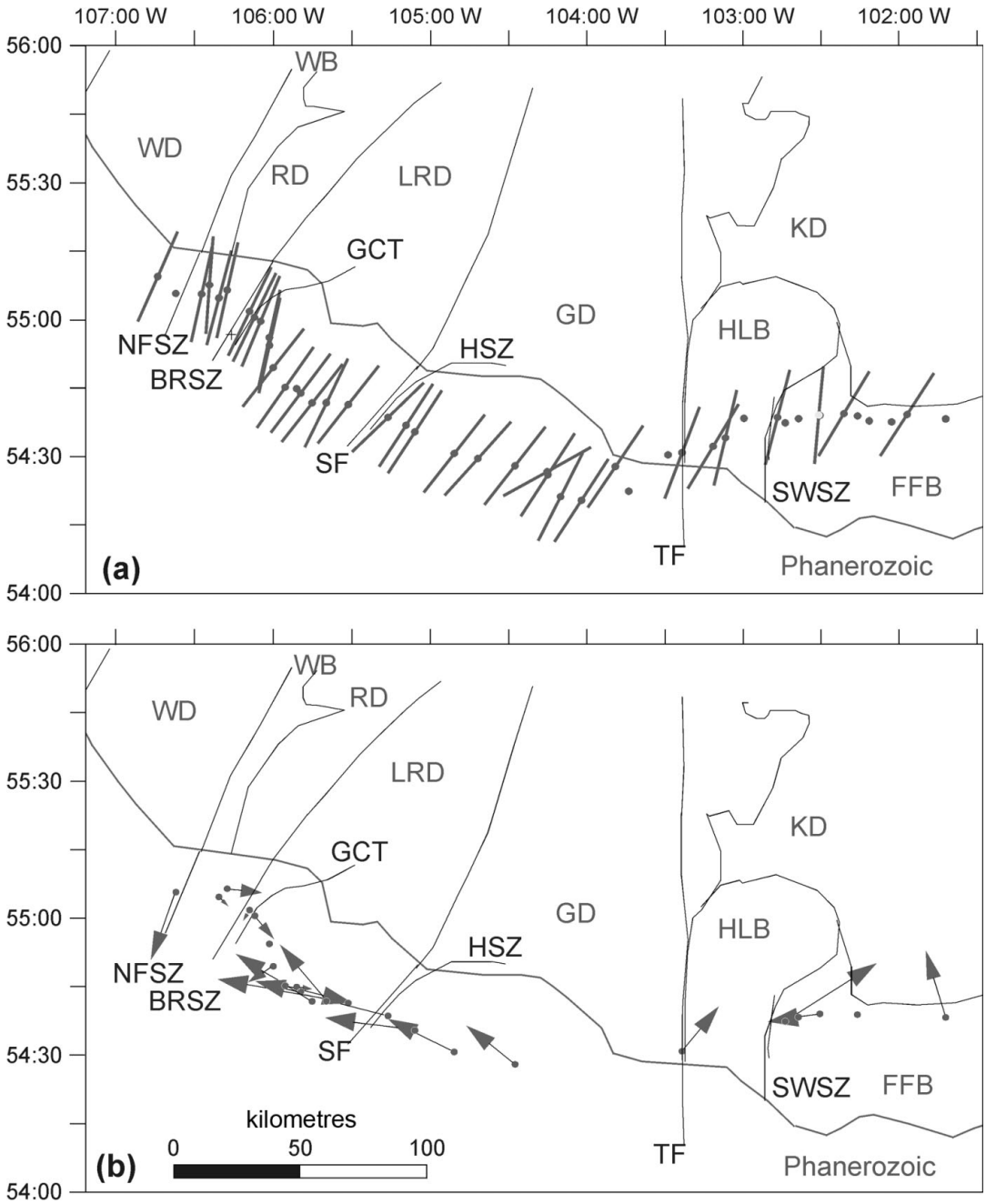

location in the west of the Glennie domain and becomes thinner to the east and to the west. This conductor is visible as low values of apparent resistivity at short periods in the TE and TM response. In the phase response, the transition from the surface conductor to more resistive rocks at greater depth creates a zone of low phase. This surface conductor can be readily attributed to the Phanerozoic sedimentary rocks occurring along the profile. The thickening of the surface conductor reflects the increasing distance of the MT transect from the shield margin.

There is a lateral change in the phase response within the La Ronge domain indicating the presence of relatively conductive rocks in the Precambrian crust beneath the surface sedimentary rocks. The effect of these conductive rocks can also be seen in the apparent resistivity pseudosection. These responses are observed most clearly in the TE components

Fig. 6. TE and TM apparent resistivity and phase sections for east–west profiles across the study area. Left panels show the observed responses and right panels show the responses of a 2-D resistivity model fitted to the data. The locations of data points used in the contouring are indicating using "+" symbols. Areas with no coverage have been blanked out. The location of Precambrian geological units and structures is indicated using the bar at the top of each set of panels. NFSZ, Needle Falls shear zone; see Figs. 1 and 2 for other abbreviations.

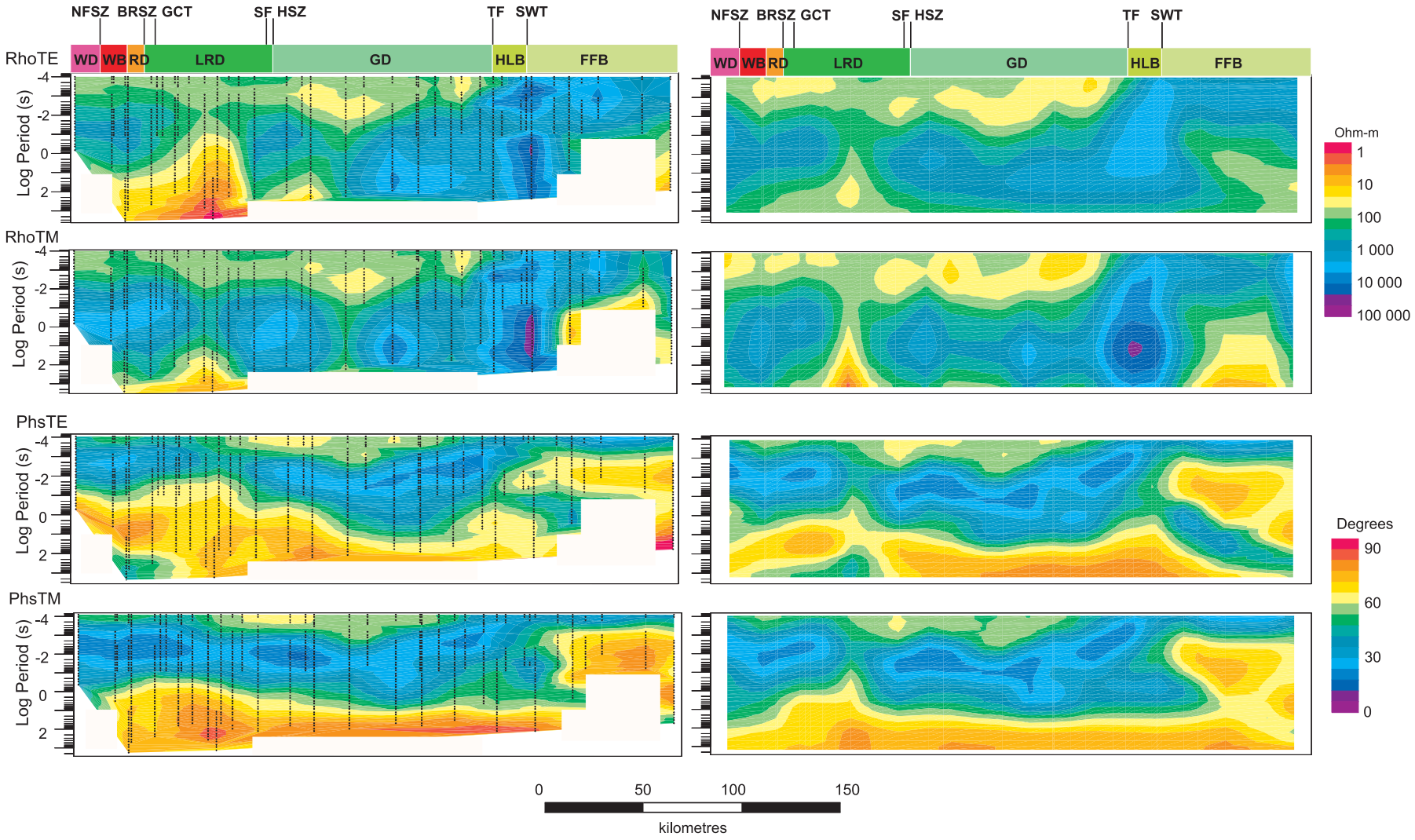

but are also visible in the TM component. Comparison of the results with those of previous studies (e.g., Jones et al. 1993) indicates the observed responses are due to the NACP conductor. The TE apparent resistivity and phase response indicate the presence of a second lobe of enhanced conductivity on the eastern margin of, and at longer period than, the main NACP response.

The shortest period response at sites east of the Tabbernor fault is more resistive than further west, as is expected for sites located on the Precambrian shield. At periods $< 10^{-3}$ s, the phase values are relatively low indicating that at shallow depths the crust becomes more resistive with increasing depth.

Inversion of MT responses and resistivity models

Methods

The MT data were fitted using 1-D and 2-D inversion methods. 1-D inversions were used to determine the resistivity structure of the Phanerozoic sedimentary rocks and employed the method of Fischer (Fischer et al. 1981). This method fits the data using a model containing the minimum number of layers that can be justified by the statistical fit to the data.

The 2-D inversions presented here employed the non-linear conjugate gradient (NLCG) algorithm of Rodi and Mackie (2001). The algorithm, which is based on a finite-difference forward modelling code, minimizes an objective function incorporating the misfit between the model response and observed data and the roughness of the model. Many different 2-D inversions were run to investigate the range of models that could fit the data and the resolution of the model.

In an initial set of inversions, 2-D models were obtained by fitting the TE and TM data for a total of 39 BBMT and AMT sites and 43 frequencies between 10^{-4} s and 263 s. In the inversions, the uncertainty on the phase response was set to a floor of 5% and the uncertainty on the apparent resistivity response was set to a floor of 20% (corresponding to an impedance error of 10%). The inverted data were not corrected for galvanic distortion so the error floor on the apparent resistivity response was set to a higher value than for the phase response to accommodate distortion. Inversions were run for a range of values of the tau factor, which controls the balance between fitting the data and minimizing departures from the starting model. Inversions were also run for a range of starting models, each consisting of uniform half-space. Finally, each inversion was restarted after its initial termination in order that the final model obtained represented a deeper minimum of the objective function. The inversions all provided models with a relatively poor fit to the data, for example, a final normalized root-mean-square (rms) misfit of 3.89 was obtained for an inversion using a tau factor of 10 and a starting model of 2000 Ω·m. This misfit is significantly higher than the statistically appropriate value of 1.0.

In a second suite of inversions, the data sets were modified to allow improved fitting of a 2-D model. Six sites that had excessively high misfits values (normalized rms > 4.0) were excluded (M41, A24, A22, M16, A16, A13). The error floor for the apparent resistivity response was also increased to 80% to more fully accommodate distortion effects in the response. Note that this change artificially reduces the normalized rms misfit result by a factor of about 2 from its previous measure. Data sets consisting of the TE response, the TM response, and the combined TE+TM response were inverted. Inversion models obtained using a starting model of 1000 Ω·m and a tau factor of 10 yielded normalized rms misfits of 1.25, 1.06, and 1.40, respectively, for the TE data, TM data, and TE+TM data sets. The resistivity model derived from the TE+TM inversion is used as the primary model for subsequent misfit evaluation and geological interpretation.

The misfit between the responses of the final 2-D model and the observed data exceeds the level appropriate for the estimated errors. Figure 6 compares pseudosections of the observed data and model responses, and Fig. 7 compares the phase responses at six representative sites. The data fit is relatively poor, particularly at sites such as M23 and M13 that have higher rms misfits. However, it is of note that the model responses do reproduce the large-scale features of the observed responses (Fig. 6). The misfit is distributed fairly evenly across the profile (Fig. 7*b*), although it does exceed the average level at most sites in the westernmost 75 km. The observed misfit of the 2-D resistivity model increases the importance of defining the degree of resolution of the features in the model, as is done in the following section.

Resistivity structures

Figure 8 shows the final 2-D (TE+TM) resistivity model at three vertical scales. The images provide an overview of the resistivity structure of the central Reindeer Zone and reveal a number of significant features.

Conductive Phanerozoic rocks

The MT model shows the Phanerozoic rocks form a conductive surface layer (labelled A in Fig. 8) with resistivity between 10 and 100 Ω·m. Comparison of 2-D and 1-D inversion models (not shown here) supports this result. The 2-D NLCG model provides limited resolution of the thickness of the conductive layer because of the smoothing used in the inversion algorithm. In contrast, the 1-D Fischer inversion models allow abrupt transitions in resistivity between adjacent layers and provide superior resolution of the base of the conductive layer. The 1-D models indicate that the sedimentary rocks reach a maximum thickness of around 100 m.

The NACP conductor

The NACP conductor consists of two conductive bodies, both labelled B in Fig. 8. This structure closely resembles that determined by Jones et al. (1993) using the RRI (rapid relaxation inversion) algorithm of Smith and Booker (1991) with a slightly different strike direction of E22°N. The geometry of the deeper conductive block is not as well defined as that of the shallow block. In inversions using a lower tau value, which fit the data more closely, the western block appears as a distinct conductor centred on 15 km depth. In inversions in which the data are not fitted as closely, the conductor is more diffuse and merges with a more extensive lower crustal conductor. At sites located above the NACP conductor, both the rms misfit (Fig. 6) and the skew at periods exceeding 1 s are relatively high (Fig. 4), suggesting that the NACP conductor may be more complex than a simple 2-D body.

Conductive lower crust beneath the western Glennie domain

The lower crust beneath the western part of the Glennie domain (labelled C in Fig. 8) has a conductivity of < 80 Ω·m. This structure is a robust feature of the resistivity model. It is improbable that this is a spurious model feature caused by a 3-D element of the resistivity structure, e.g., the edge of the Phanerozoic rocks or a finite strike of the NACP conductor, because it appears in the separate inversions of the TE data, TM data, and joint data set. To further test the existence of the conductive lower crust an inversion was run in which the lower crust was constrained to be resistive. The resistivity of the crust between 20 and 40 km depth between sites M28 and M23 was constrained to 1000 Ω·m. The normalized rms misfit of the resulting model (1.55) was 10% higher than for the unconstrained model and as shown in Fig. 7 the increased misfit extended fairly systematically across 10 adjacent sites in the profile. The results indicate that the conductive lower crust is a feature required by the MT data and that it is not a spurious feature caused by localized 3-D responses in the data. The conductive lower crust also appears in resistivity models obtained using different algorithms, e.g., 1-D modelling by Jones and Correia (1992) and 2-D modelling using the RRI algorithm (Grant 1997*b*).

Extension of lower crustal conductor

The upper surface of the lower crustal conductor is at a depth of around 25 km in the west, but an extension of the conductor (labelled D on Fig. 8) rises into the upper crust towards a location about 40 km east of the Hartley shear zone. This feature is evident in Fig. 8 but is more prominent in models fitted using a lower tau value. The shallow part of the conductor is related to the apparent resistivity and phase anomaly adjacent to the NACP anomaly in Fig. 6.

Upper crust beneath the Glennie domain and Hanson Lake block

The shallow crust beneath the westernmost Glennie domain is relatively resistive and includes a zone in which resistivity values exceed 1000 Ω·m (labelled E on Fig. 8). There are several moderately conductive features in the uppermost 20 km of crust beneath the Glennie domain, such as feature D and the shallow conductive zone located 40 km west of the Tabbernor fault. These features appear in most inversion models and are considered quite well resolved. The resistivity model for the uppermost crust beneath the Hanson Lake block includes a relatively resistive thin surface layer (>1000 Ω·m) overlying a more conductive region. Considering the site spacing, the proximity to the edge of the Phanerozoic cover, and the relatively high skew in this part of the profile, it is unlikely that these shallow structures are fully resolved.

Middle and lower crust beneath the central Glennie domain to western Flin Flon belt

Much of the middle and lower crust beneath the central Glennie domain, Hanson Lake block, and western Flin Flon belt is relatively resistive (labelled F on Fig. 8) with resistivity in the range 1000–5000 Ω·m. The high resistivity is related to low phases noted at periods of 0.01–0.1 s at a number of sites (Fig. 6).

Dipping conductor beneath Flin Flon belt

The resistivity structure of the uppermost crust in the western Flin Flon belt includes a relatively conductive layer that dips to the east (labelled G in Fig. 8). The geoelectric strike for this part of the profile is poorly resolved and the skew angle is high indicating that this part of the model should be interpreted with care. However, the dipping conductor appears in inversions of the individual TE and TM data sets, as well as in inversions of the joint data set suggesting that the feature is a true structure.

Spurious features of the 2-D resistivity model

The lower crustal conductor appearing beneath the Flin Flon belt (labelled H in Fig. 8) does not occur in inversions of the TE data set. It is interpreted to be a spurious feature in the 2-D model caused by the presence of 3-D structures near the eastern end of the profile. As noted earlier in the text, such features would explain the relatively large skew values noted in this part of the profile (Fig. 4). The MT method provides limited resolution of moderately conductive zones occurring beneath more shallow conductors, such as the parts of the 2-D resistivity model beneath the NACP conductor, beneath the near-surface conductor in the eastern Glennie domain, and immediately beneath the dipping conductor in the Flin Flon belt (Fig. 8). These features may be spurious elements of the 2-D resistivity model, caused by smearing of enhanced conductivity from adjacent conductive zones into regions of limited MT resolution.

Comparison of resistivity models and seismic results

Seismic reflection profiles from the Lithoprobe transect have shown that the internal zone of the THO has been subjected to thick-skinned style deformation with significant dipping reflective zones extending from the surface to Moho depths (Lucas et al. 1994; White et al. 1994; Lewry et al. 1994). To the west of the Glennie domain, the response is characterized by west-dipping packages of reflectors extending through the crust and within the Glennie domain, and further east, the response is characterized by east-dipping packages (Fig. 9). In the upper crust, the transition from west to east dips occurs in the western Glennie domain. This location is underlain by a distinct, 50 km-wide crustal root. Across most of the profile, there is a distinct Moho reflection at around 12 s (~38 km) that separates highly reflective crust from almost transparent mantle (Lewry et al. 1994). At the crustal root, this reflection deepens to around 15 s (~48 km). Fig. 9 compares the seismic reflection response and resistivity models for the whole study area, and Fig. 10 compares the results from two smaller regions in more detail.

NACP conductor

Figure 10*a* compares the seismic reflectivity and resistivity model in the area of the NACP. The Lithoprobe Vibroseis seismic reflection data in this area are described by Lewry et al. (1994) and have been analysed in detail by Hajnal et al. (1996) and Hajnal et al. (2005) to better delineate the tectonic structures. The results of Vibroseis and dynamite surveys are compared by Bezdan and Hajnal (1996), and the Moho has been imaged in using wide-angle reflections by Németh et

Fig. 7. (*a*) Comparison of observed and model TE and TM phase responses at six sites along the MT profile. The model response is for the model obtained from the TE+TM data. The location of the sites and the rms misfit are shown in part (*b*). (*b*) Normalized rms misfit at sites along the MT profile for the TE+TM model. The misfit is shown for an unconstrained model and for a model in which the lower crust between sites M28 and M23 is constrained to be resistive (1000 Ω·m). The rms values are for 5% phase and 80% apparent resistivity error floors. CLC, conducting lower crust.

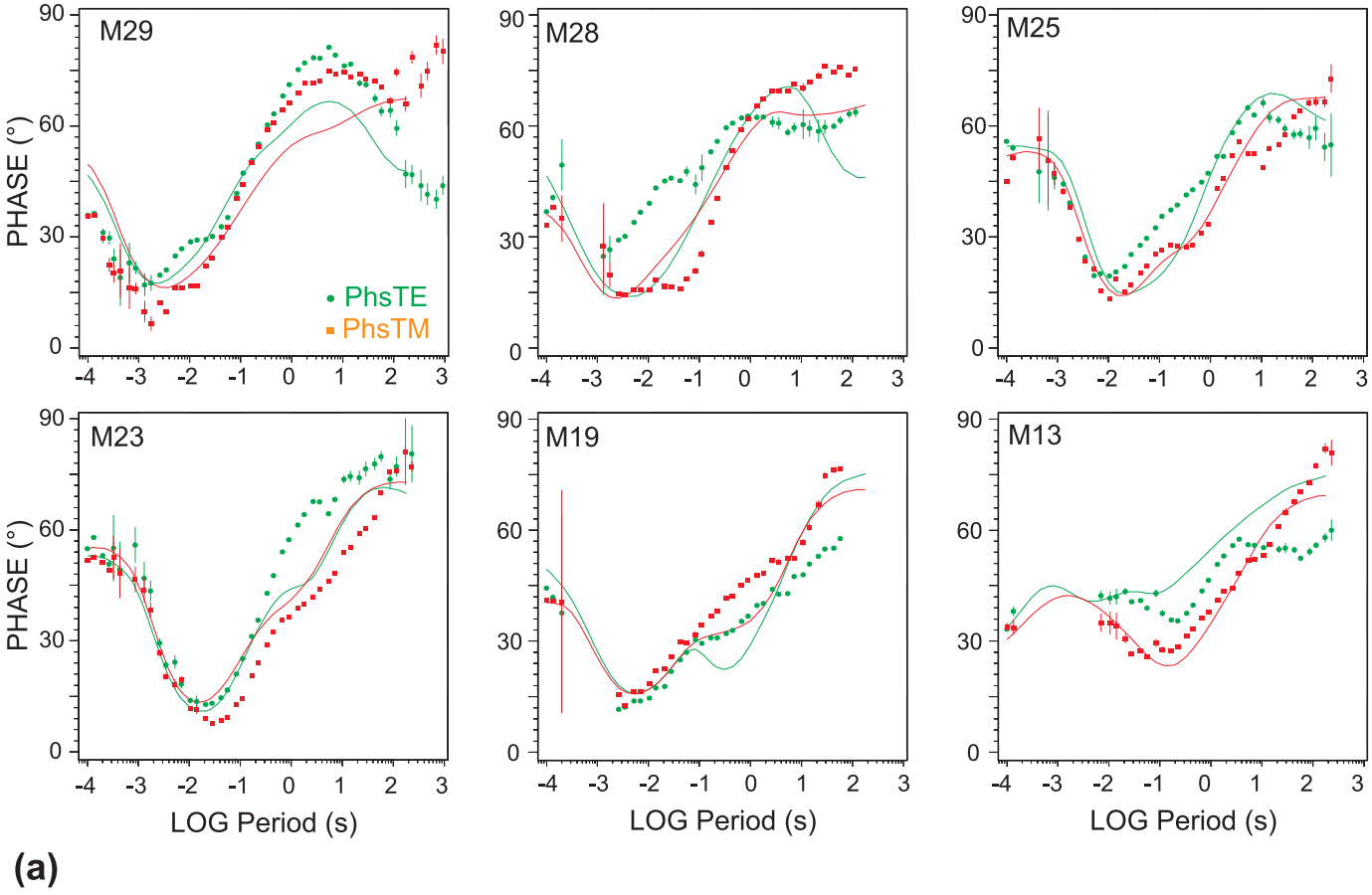

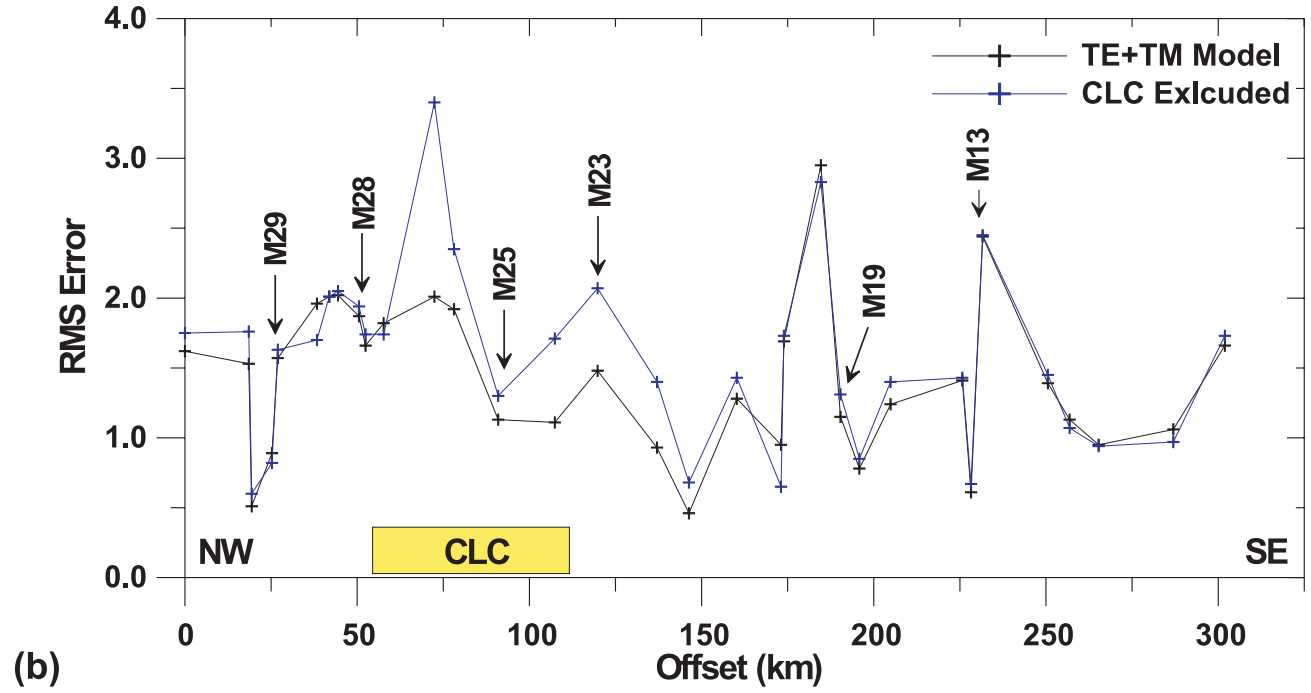

Fig. 8. Resistivity sections derived obtained from 2-D inversions of the TE and TM data using the NLCG algorithm. Blue and red tics at the top of each panel indicate the location of MT and AMT sites respectively and green tics indicate the location of sites removed from the final inversions. The upper panel shows the uppermost 500 m of the resistivity structure and the corresponding bar shows the surface geology. Orw, Ordovician Red River and Winnipeg Formations; Km, Cretaceous Mannville Group; Kic, Cretaceous Lower Colorado Group. The middle panel shows the uppermost 5 km of the resistivity structure at a vertical exaggeration of ~10:1. The lower panel shows the resistivity structure of the crust and uppermost mantle with a vertical exaggeration of ~0.3. NFSZ, Needle Falls shear zone; see Figs. 1 and 2 for other abbreviations. Labelled features A–H are discussed in the text.

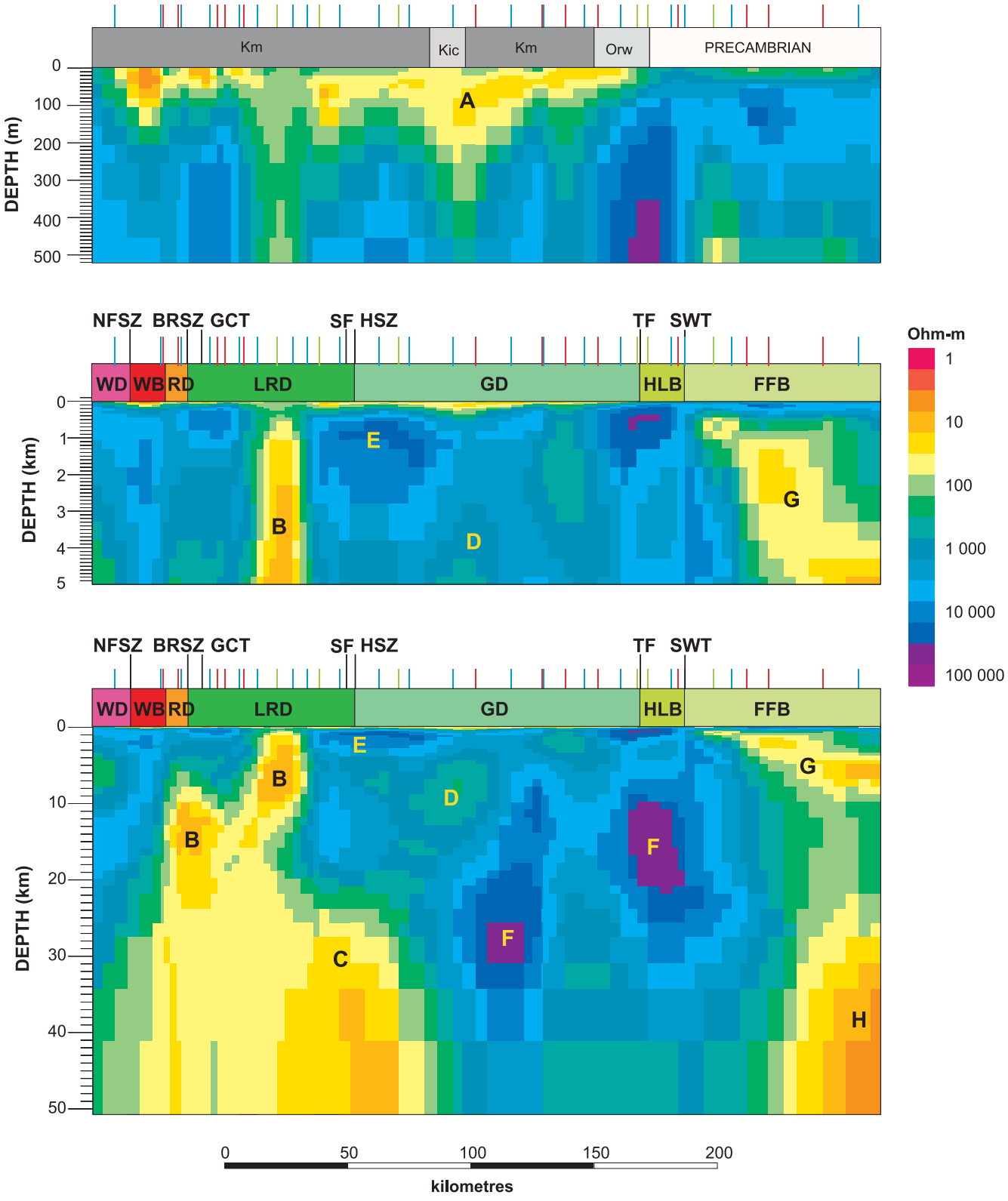

Fig. 9. (*a*) Seismic reflectivity along line 9 of the Lithoprobe THO Transect (from Lewry et al. 1994). (*b*) Comparison of resistivity and reflectivity across the study area. The overlay of the two data sets is based on a seismic velocity of 6 km s^{-1}. Regions in which there is little or no resolution of the resistivity have been blanked. M, Moho; SC, Sask craton; CLC, conducting lower crust; NFSZ, Needle Falls shear zone; see Figs. 1 and 2 for other abbreviations.

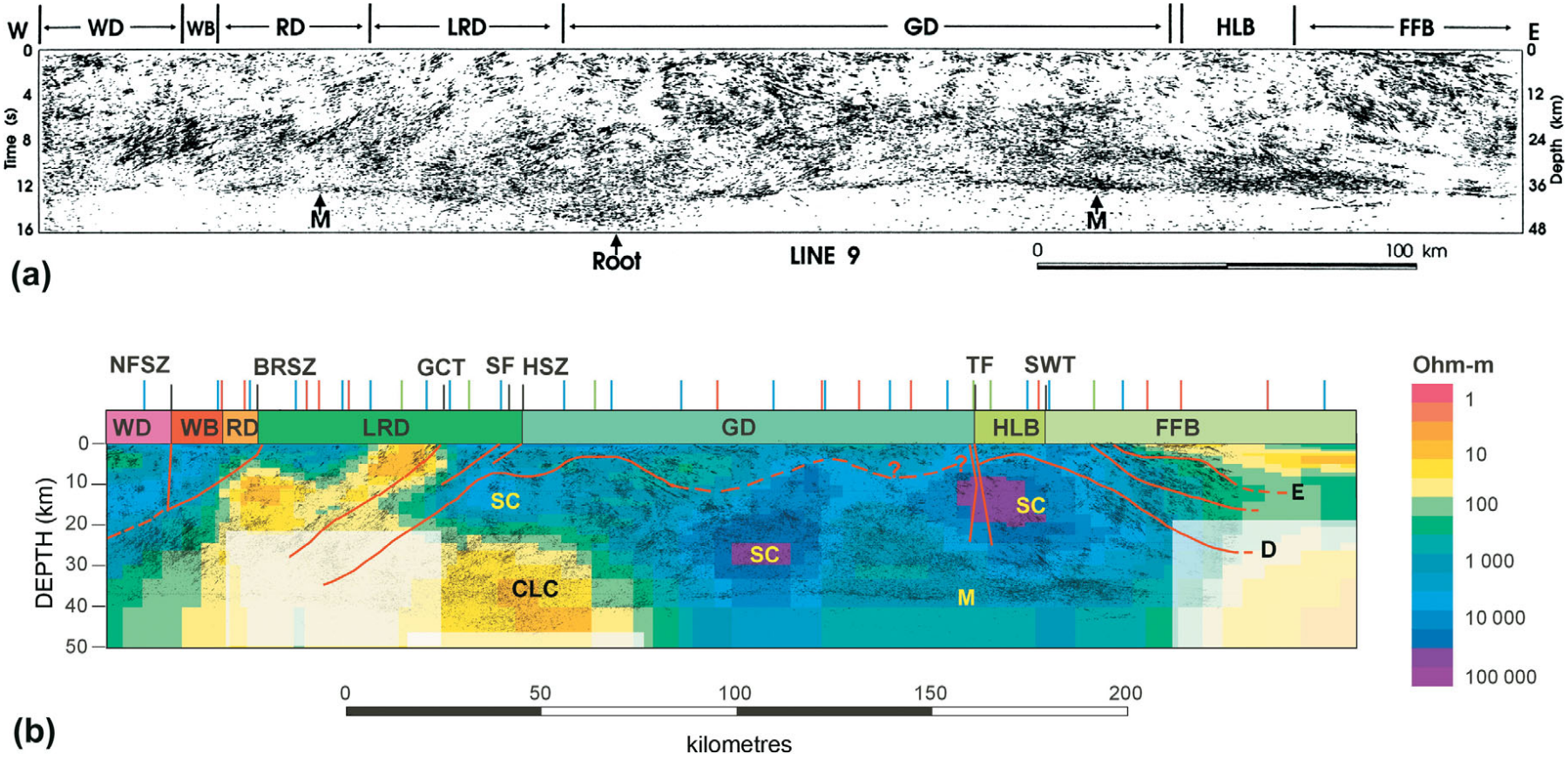

Fig. 10. Comparison of seismic reflection and structures interpreted from the seismic data with resistivity data. The overlay of the reflectivity and resistivity data sets is based on a seismic velocity of 6 km s^{-1}. (*a*) Western part of study area (seismic data from Hajnal et al. 1996). Four interpreted locations of the Guncoat thrust are shown: 1, from Hajnal et al. (2004); 2, from Lewry et al. (1994); 3, from Baird and Clowes (1996); 4, from Jones et al. (1993). PC1 and PC2, upper and lower limits of a distinct band of reflectivity interpreted to correspond to the upper surface of the Sask craton; R, crustal root; UF, unnamed fault; M, Moho; CLC, conducting lower crust; (*b*) Eastern part of study area (seismic data from Pandit et al. 1998). PT, Pelican thrust; E, detachment within Flin Flon belt rocks; D, deeper detachment; M1, Moho; M2, sub-Moho reflections. The detachment D is interpreted to be the upper surface of the Sask craton. Its location is based on the location of characteristic reflections PC1 and PC2 identified in the west of the profile (Hajnal et al. 2004), the location of the Pelican thrust in the east of the profile (Pandit et al. 1998), and (where dashed) the upper limit of resistive regions in the centre of the profile. See Figs. 1 and 2 for other abbreviations in (*a*) and (*b*).

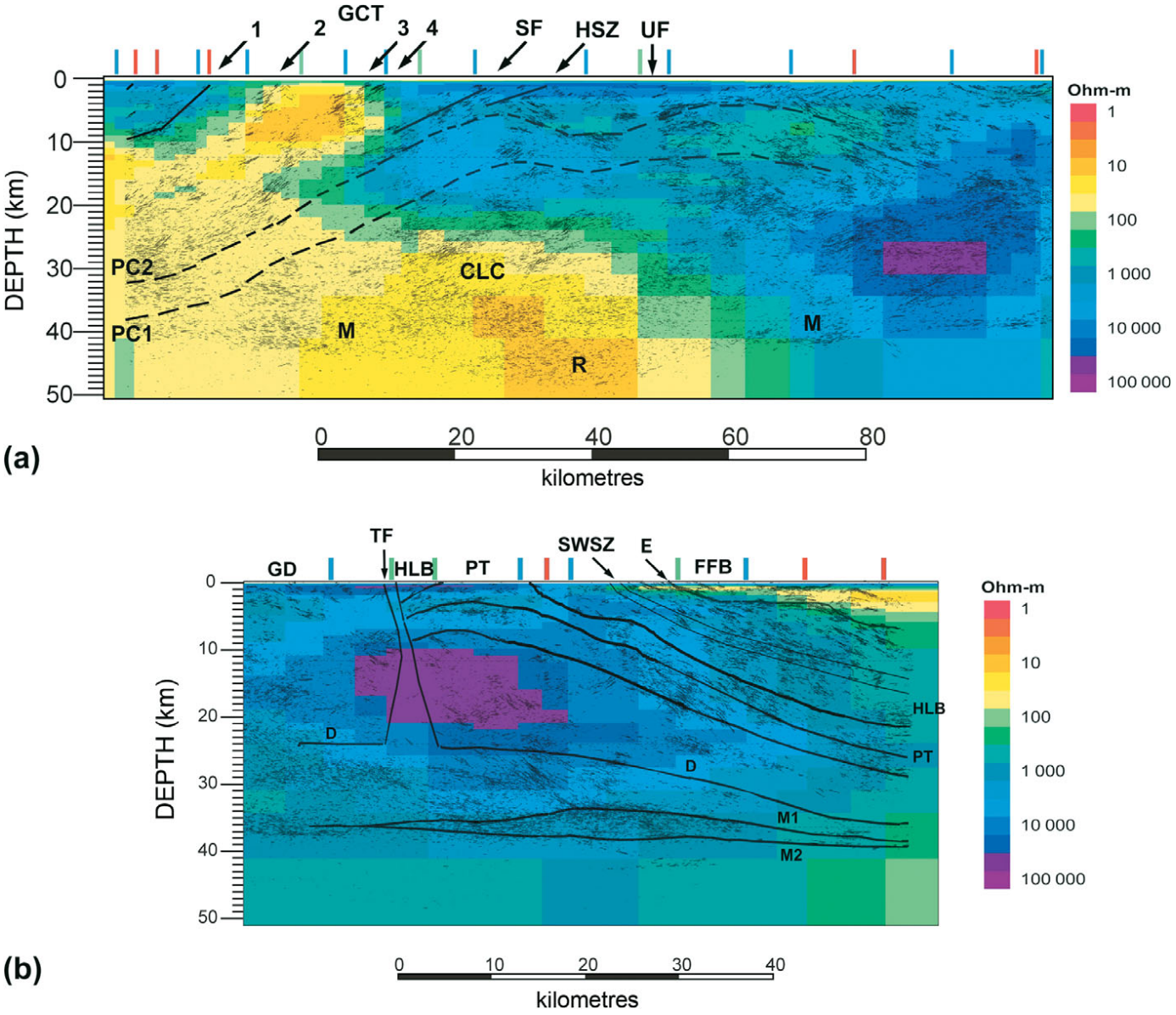

al. (1996). As noted by Jones et al. (1993), the NACP conductor lies within westward dipping reflectivity and tracing of the reflections updip to the surface indicates that the conductor lies within the rocks of the La Ronge domain. More detailed interpretations of the NACP conductor are given in Jones et al. (1993) and Jones et al. (1997*a*, 2005). The NACP conductor is interpreted to be bounded above by the Birch Rapid straight zone and below by the Guncoat thrust, with its western extent limited by the Needle Falls shear zone. In this interpretation, the conductor lies within the Wapassini sheet of Lewry et al. (1990).

Because the Lithoprobe seismic reflection and MT profiles lie to the south of the exposed shield, there is some uncertainty in the delineation of the geological sub-unit hosting the NACP conductor. This uncertainty is related to the extrapolation of the Guncoat thrust from the exposed shield at the latitude of the Lithoprobe line (Fig. 10). Hajnal et al. (2004) place the thrust at the location marked 1 on Fig. 10*a*, based primarily

on interpretation of the seismic reflection data. However, they note that this positioning is somewhat problematic. Lewry et al. (1994) show the thrust ~10 km further east of the previous position, at the location marked 2 on Fig. 10*a*. On the basis of potential-field data and careful interpretation of the seismic reflection data, Baird and Clowes (1996) position the thrust further east again, at location 3 on Fig. 10*a*. In this location, the Guncoat thrust would form the upper surface of the NACP conductor (Fig. 10*a*). This geometry would mean the NACP conductor was located within the Guncoat gneisses. The Wapassini sheet is stratigraphically above the Guncoat thrust so for the NACP to lie in the Wapassini sheet, the Guncoat thrust must pass to the east of and below the NACP conductor. This location for the thrust is marked as 4 on Fig. 10*a* and is the location interpreted by Jones et al. (1993).

Examination of the lithologies involved supports the interpretation of Jones et al. (1993). In Precambrian terranes, a common source of enhanced conductivity is sulphidic or graphitic pelitic metasedimentary rocks. The rocks of the Wapassini sheet are derived from highly migmatized pelitic gneisses and pelite diatextite protoliths and provide a probable source of conductive rocks. Analysis of pelitic rocks from the Wapassini sheet confirms the presence of conducting sulphides (Jones et al. 1997*a*). It is not possible to exclude a contribution to the conductor from graphitic rocks that occur in the Guncoat thrust (Katsube et al. 1996). However, it is less likely that there is a contribution to the conductor from the underlying Cartier sheet (Glennie domain), which is derived mainly from dioritic to granitic protoliths and contains only subordinate pelitic gneisses (Lewry et al. 1990).

Westernmost Glennie domain

The Stanley fault has most recently been interpreted to be a west-dipping structure (Fig. 2 in Hajnal et al. 2004), but in earlier studies, it was interpreted to form a steeply dipping structure penetrating to at least 4 s depth (Hajnal et al. 1996). The Stanley fault lies within a relatively resistive part of the resistivity model so the MT results provide no evidence to discriminate between the two seismic interpretations. Similarly, the resistivity models provide no resolution of the Hartley shear zone.

The resistivity data support the interpretation of a subvertical fault located around 20 km east of the Stanley fault. At this location a zone of poor reflectivity extends to 5 s (15 km) and possibly 8 s (24 km) depth (Fig. 10). Hajnal et al. (1996) comment that the steeply inclined transparent zone has not been linked to a known fault at the surface. The transparent zone lies near the western margin of a zone of enhanced conductivity extending between about 5 and 15 km (feature D in Fig. 8). Considering the resolution of MT data, it is probable that the transparent zone coincides with the western margin of the conductive zone. Taken together, the seismic and resistivity results support the presence of a significant fault at this location.

The very resistive near-surface zone to the east of the NACP conductor (feature E in Fig. 8) extends from ~10 km west of the Stanley fault to around ~20 km east of the fault and penetrates to depths of around 5 km. It is of note that the Nistowiak and Hunter Bay windows of exposed Archean rocks occur along strike from this resistive zone, ~50 km north of the Lithoprobe transect (Fig. 2).

Glennie domain

Isotopic evidence suggests the Glennie domain is underlain by Archean rocks: drill-core samples from south of the Lithoprobe transect have yielded Sm–Nd model ages of 2.35–3.33 Ga (Chiarenzelli et al. 1996). The seismic reflection data for the segment of the Lithoprobe transect crossing the Glennie domain define a regional detachment at the base of the unit that is interpreted to separate the Proterozoic rocks from the underlying Sask craton. In the west of the Glennie domain, the upper boundary of the Sask craton is defined by a characteristic band of reflectivity (between PC1 and PC2 on Fig. 10*a*) (Hajnal et al. 1996). This band is correlative with the Pelican thrust, which forms the basal detachment zone of the juvenile Proterozoic rocks east of the Tabbernor fault (Fig. 10*b*). The resistivity model shows that the detachment surface beneath the western Glennie domain separates rocks containing a number of zones of moderate conductivity (~100 Ω·m) from more rocks that are generally more resistive at depth (Fig. 10*a*).

There is uncertainty in the depth to the Archean basement further east in the Glennie domain (Lewry et al. 1994). Interpretations of the seismic reflection data show the detachment increasing gradually in depth to the east from a value of around 1.5 s (4 km) near the Stanley fault to 5 s (18 km) near the Tabbernor fault (Lewry et al. 1994; Hajnal et al. 1996). The resistivity model includes a region of very high resistivity in the central Glennie domain (Fig. 9*a*) that extends above this interpreted position of the detachment. The results suggests that either the Glennie domain contains a localized zone with increased resistivity or else the interface between the Glennie domain and underlying rocks is more shallow than previously interpreted in this area. Accordingly, in Fig. 9*a* the location of the detachment in the central Glennie domain is redefined on the basis of the resistivity results to separate the more conductive rocks in the upper 5 to 10 km from the more resistive rocks at depth.

The MT results provide less resolution of the position of the detachment in the eastern Glennie domain. The resistivity results suggest an increase in resistivity between 5 and 10 km depth, and there is a decrease in reflectivity at a similar depth. One interpretation of these results is, therefore, that the detachment is located at this relatively shallow depth (as shown in Fig. 9*a*). However, as discussed in the next section, the resistivity model also provides some support for the interpretation made from the seismic reflection data that the detachment is located at around 18 km depth.

Tabbernor fault

Pandit et al. (1998) reprocessed the seismic reflection data from the eastern part of the study area. The Tabbernor fault is imaged in the originally processed data (Lewry et al. 1994; Hajnal et al. 1996) and in the reprocessed data (Pandit et al. 1998) as a prominent seismically transparent zone extending to 9 s (27 km) depth with diffraction patterns on the unmigrated data, indicating truncation of reflections on either side of the zone. The resistivity model suggests that the fault zone itself does not have a significantly conductive signature. Site A16 was located within the fault zone and although the data from this site were affected by noise, requiring the removal of this site from the inversion, they

were sufficiently good to indicate a relatively resistive response (apparent resistivity values exceed 100 Ω·m).

With the removal of sites A16 and M13 from the data sets used in the MT inversions, there is insufficient site density to accurately define the western limit of a region of high resistivity (>5000 Ω·m) extending eastward from near the Tabbernor fault between 10 and 20 km depth. However, the MT data are consistent with the Tabbernor fault forming the western margin of this resistive block. This result suggests that, at upper crustal levels, the Tabbernor fault separates resistive Archean rocks to the east from more conductive rocks of the Glennie domain to the west and supports the interpretation of a detachment depth of 18 km immediately to the west of the Tabbernor fault.

Sturgeon–Weir shear zone and Pelican thrust

In earlier interpretations of the seismic reflection data, the Sturgeon–Weir shear zone was defined as a moderately steeply dipping east-dipping feature (Lewry et al. 1994; White et al. 1994; Hajnal et al. 1996). However, the reprocessing of the reflection data by Pandit et al. (1998), and particularly the application of a variable cross-dip correction, considerably improved the resolution of some sub-surface features and their correlation with the surface geology (Fig. 10*b*). It is now evident that the Sturgeon–Weir shear zone thrust dips to the east at a relatively shallow angle. The shear zone is underlain by the rocks of the Hanson Lake block, which are in turn underlain by the Pelican thrust, a several kilometre-wide high-strain zone that is interpreted to be the major detachment zone separating the allochthonous Proterozoic rocks from the underlying Archean rocks.

The resistivity model for this region includes a conductor (with resistivity of < 100 Ω·m) that dips to the east from a near-surface location in the western Flin Flon belt (feature G in Fig. 8). The base of this feature appears to correlate with a zone of high reflectivity within the Flin Flon belt rocks (labelled E on Fig. 10*b*). Although the MT method can provide only limited resolution of the base of a conductor, the dipping conductor appears to lie well above the Sturgeon–Weir shear zone. Ferguson et al. (1999) previously interpreted the presence of relatively high upper crustal conductivity in the northwest part of the Flin Flon belt and suggested that the enhanced conductivity may be associated with graphitic–sulphidic rocks of the Namew gneiss complex. The MT method provides poor resolution of resistive structures underlying more shallow conductive rocks and so provides insufficient resolution to discriminate the Hanson Lake block, Pelican thrust, and underlying Archean rocks.

Lower crustal conductor

The middle to lower crustal conductor in the west of the Glennie domain (Figs. 9, 10) is a well-resolved feature of the resistivity model. It has not been defined in resistivity models determined from MT profiles further south in the THO, but the resolution of such a feature in these locations would be limited by the overlying conductive sedimentary rocks of the Williston basin. These rocks have an integrated conductance of 300 S or more (e.g., Jones 1988), sufficient to cause a significant decrease in the resolution of underlying crustal resistivity structure. A second Lithoprobe MT profile to the north did not extend sufficiently far into the Glennie domain to indicate whether the conductive crust extended to the north (Jones et al. 1997*a*).

The lower crustal conductor lies within the core of crustal culmination defined by the seismic reflection data and cuts horizontally across strong west-dipping reflectivity. The conductive zone lies within part of the crust that has been interpreted to consist of Archean rocks. However, elsewhere in the THO, in the vicinity of the Pelican, Nistowiak and Hunter Bay windows, rocks with more definite Archean affinity are observed to be relatively resistive. Jones et al. (1997*b*) have suggested that the lower crustal conductor in the Glennie domain indicates the presence of Proterozoic rocks in the lower crustal of the Glennie domain, contradicting the interpretations of the seismic results.

In most areas of the Canadian Shield, Archean crust has relatively high resistivity (e.g., Boerner et al. 2000; Jones and Ferguson 2001; Jones et al. 2002; Ferguson et al. 2005). Relatively conductive Archean crustal rocks are generally observed on only a relatively small scale e.g., within narrow greenstone belts and in shear zones (e.g., Boerner et al. 2000), in some metasedimentary sequences (e.g., Ferguson et al. 2005), and in some suture zones (Jones et al. 2002). On this basis, it is improbable that a large volume of Archean crust of the Sask craton is inherently conductive, suggesting that the enhanced conductivity of the lower crust beneath the western Glennie domain is explained by either later alteration of Archean rocks or by the presence of younger rocks.

There is considerable evidence indicating significant post-Archean deformation and alteration of the Sask craton crust and the underlying lithosphere, so it is necessary to assess whether the processes involved might have enhanced the conductivity of the lower crust. Seismic reflection results provide evidence for at least two generations of Moho beneath the Glennie domain (Bezdan and Hajnal 1996; Németh et al. 1996). Hajnal et al. (1996) attribute the formation of the more shallow Moho reflections to post-collisional deformation in the THO. However, this process seems unlikely to have introduced the necessary conducting constituents (carbon, sulphides, or oxides) into the Archean rocks at sufficient scale to explain the enhanced lower crustal conductivity.

The mantle beneath the Glennie domain is anomalous. Seismic refraction – wide-angle reflection surveys have defined an anomalous high-velocity zone in the uppermost mantle extending 100 km north–south by 130 km east–west with a maximum thickness of 50 km (Hajnal et al. 1997). This high velocity zone is interpreted to be an eclogitic zone formed in the mantle following collisional processes or subduction events (Bezdan and Hajnal 1996). Dipping reflections in the lower crustal root can be traced down-dip into the upper mantle (Bezdan and Hajnal 1996). The fact that these reflections are parallel to Proterozoic crustal structures suggests the slabs were initially emplaced during Proterozoic events, and therefore the eclogitization was also a Proterozoic process. Jones et al. (2004) have also shown that the upper mantle beneath the region of the conductive lower crust is anomalously conductive. It is possible that fluids released during dehydration reactions associated with eclogitization could have affected the conductivity of the crust and mantle, but the geometry of the enhanced conductivity does not support this interpretation. Within the mantle the highest

conductivity occurs at depths > 80–100 km and not immediately beneath the Moho. Also, within the crust the location of the enhanced conductivity is partially offset from that of the mantle velocity anomaly and the crustal root (Németh et al. 1996; Hajnal et al. 1997). The high conductivity extends asymmetrically across only the western two-thirds of the mantle root, suggesting that it is unlikely that fluids derived from eclogitization caused the observed lower crustal conductivity.

On a larger scale, tomographic inversions of teleseismic data suggest that the lithosphere western Glennie domain at the latitude of the Lithoprobe transect is underlain by a region of relative slow *P*-wave velocity at 100–200 km depth (Bank et al. 1998). There is good spatial correlation between the low-velocity anomaly at 100 km, which is spatially well resolved by the teleseismic data (Bank et al. 1998), and the enhanced lower crustal conductivity. The velocity structure is interpreted to be due to thermomechanical erosion of the lithosphere by a small-scale convection instability or plume at 100 Ma, an interpretation supported by the presence of Cretaceous diamondiferous kimberlites (Bank et al. 1998). Although such a mantle event could conceivably have produced fluids that interacted with the overlying crust it does not seem to provide a good explanation for the observed enhanced conductivity in the lower crust. As for the Proterozoic eclogitization event, it is difficult to see how a Cretaceous mantle plume event could explain the relatively small lateral scale of the enhanced conductivity in the lower crust and the vertical distribution of enhanced conductivity within the upper mantle.

An alternative interpretation of the lower crustal conductor, as first suggested by Jones et al. (1997*b*), is that at least part of the lower crust beneath the Glennie domain is of Proterozoic age. Considering the occurrence of the enhanced conductivity at the edge of the Archean block a possible source of enhanced conductivity is Proterozoic ocean margin sediments of the Sask craton. Oceanic margin rocks from both the adjacent Rae–Hearne craton and Superior craton have relatively high conductivity. In the case of the Rae–Hearne craton, Jones et al. (1997*a*) and Jones and Kalvey (1993) report occurrences of relatively high conductivity in the Wollaston domain and, in the case of the Superior craton, White et al. (2000) describe relatively high conductivity in the Thompson Belt in the Superior boundary zone. Support for this interpretation also comes from isotopic dating of rocks from the Archean windows (Chiarenzelli et al. 1996) and drill-core samples from further south in the THO (Baird et al. 1996) which provide evidence of rocks with both Archean and Proterozoic affinities.

A less probable source of the enhanced conductivity is juvenile Proterozoic rocks incorporated into the lower crust beneath the Glennie domain. Based on the surface geometry of the tectonic units described earlier in the text, it would be most likely that conductive rocks were of the Cartier sheet. The resistivity structure of the upper crust shows that although the rocks of this thrust sheet are not as conductive as the rocks of the Wapassini sheet, but they are more conductive than the Archean rocks. As noted earlier, the Cartier sheet does contain minor pelitic gneisses. An interpretation of the lower crustal conductor in terms of juvenile Proterozoic rocks would require the subsurface geometry beneath the western Glennie domain to be considerably more complex than previously interpreted. The Archean crust beneath the Hunter Bay and Nistowiak windows would form a discrete block separated from the main part of the Sask craton by the Stanley fault and the unnamed fault to the east. It is of note that the Bouguer gravity anomaly along the Lithoprobe transect does contain 10 km-wide, 10–20 mGal (1 Gal = 1 cm s^{-2}) negative and positive peaks at the western margin of the Glennie domain that are not explained by the traditional interpretation of the seismic reflection data (Thomas and Tanczyk 1993).

Conclusions

The MT data, collected at sites in the central Trans-Hudson orogen during 1992, image a collisional zone in which Proterozoic arc-related rocks have been juxtaposed against Archean rocks of the Sask craton. The electrical conductivity structure is relatively complex with 3-D elements at depth and near the northern margin of the Flin Flon belt. The MT data define a dominantly 2-D structure over much of the profile for periods between 0.01 s and 100 s, with a mean geoelectric strike direction of N28°E.

Images of the crustal resistivity structure have been produced using MT data from 39 sites using a 2-D NLCG inversion algorithm. The resistivity images reveal that regions interpreted to be Archean in age are relatively resistive (>2000 Ω·m). Highly resistivity regions occur at depth beneath the Hanson Lake block, beneath the central Glennie domain, and in the uppermost crust beneath the westernmost Glennie domain. Regions of crust dominated by Proterozoic arc rocks are generally more conductive (100–1000 Ω·m), including rocks of the Flin Flon belt, the Glennie domain, and the La Ronge domain. The MT results define the location of the NACP conductor within the La Ronge domain. For the conductor to lie in the geological sub-unit most likely to contain electrically conductive rocks (the Wapassini sheet), it is necessary that at the latitude of the Lithoprobe profile, the Guncoat thrust is located to the east of the position interpreted from seismic reflection data. The MT results also provide support to seismic reflection evidence for the presence of an unnamed subvertical fault about 20 km east of the Stanley fault.

A significant aspect of the resistivity model that cannot be explained directly by the seismic results is a conductive lower crust beneath the western Glennie domain. If these rocks are of Archean age, as interpreted from seismic data, it is most likely that the enhanced conductivity is due to post-Archean modification of the rocks. Such processes could have occurred during the Proterozoic deformation, subsequent eclogitization of the uppermost mantle lithosphere, or during postulated thermomechanical erosion of the lithosphere in the Cretaceous. An alternative explanation is that the lower crust is more complex than interpreted from the seismic data and includes a component of Proterozoic rocks. This interpretation is supported by the geometry of the conductor, its apparent offset by a fault, and the presence of a relatively short wavelength gravity anomaly in this area. The most likely candidates for the conductor are Proterozoic sediments deposited on the margins of the Sask craton or rocks of the Cartier sheet of Lewry et al. (1990).

The results of the present study demonstrate the importance

of including MT surveys in investigation of orogens, such as the THO, that are characterized by relatively complex geology over a range of crustal depths and include marine, near-shore and continental rocks; dipping, subhorizontal and subvertical geological contacts; and structures resulting from both brittle and ductile deformation. The MT method can delineate, or aid in delineating, different geological units, particularly metasedimentary rocks containing graphite and sulphides that were deposited in restricted oceanic basin settings (e.g., the rocks hosting the NACP conductor). The method is valuable for delineating near-vertical contacts between geological units of different resistivity that may not be well resolved in seismic reflection studies (e.g., the unnamed fault east of the Stanley fault). Finally, as demonstrated by the consideration of the relative location of the NACP conductor and the Guncoat thrust in the present study, the MT method provides information complementary to that from other geophysical studies

Acknowledgments

Financial support for this project was provided by Lithoprobe, the Geological Survey of Canada, University of Manitoba (Research Grants), and the Natural Sciences and Engineering Research Council of Canada (NSERC). The data from the contracted BBMT–AMT survey were collected by Phoenix Geophysics (Toronto, Ontario) and the LMT data were collected using instruments form the Geological Survey of Canada. J. Craven, C. Farquharson, B. Roberts, and Sheng Yu assisted with the data collection. Processing of the LMT data was performed using software from the Geological Survey of Canada and presentation of the results using GEOTOOLS. X. Ma and X. Wu assisted with the 2-D inversions. B. Pandit and Z. Hajnal provided seismic results. Reviews by M. Unsworth, P. Wannamaker, and F. Cook lead to significant improvement of the manuscript.

References

Andersen, F., Boerner, D.E., Harding, K., Jones, A.G., Kurtz, R.D., Parmelee, J., and Trigg, D. 1988. LIMS; long period intelligent magnetotelluric system. *In* Proceedings of the 9th Workshop on Electromagnetic induction in the Earth and Moon. *Edited by* M.S. Zhdanov, M.N. Berdichevsky, E.B. Fainberg, and V.V. Spichak. International Association of Geomagnetism and Aeronomy (IAGA), Working Group I-2 Electromagnetic Induction and Electrical Conductivity.

Ansdell, K.M., Lucas, S.B., Connors, K.A., and Stern, R.A. 1995. Kisseynew metasedimentary gneiss belt, Trans-Hudson orogen (Canada); Back-arc origin and collisional inversion. Geology, **23**: 1039–1043.

Ashton, K.E., and Lewry, J. 1994. Vergence of the "Pelican Slide" and Sturgeon–Weir Shear Zone. *In* Trans-Hudson Orogen Transect. Report of the 4th Transect Meeting, Saskatoon, Sask., April 11–12, 1994. Lithoprobe Report 38, pp. 12–17.

Ashton, K.E., and Lewry, J. 1996. Geological history of the northern Hanson Lake Block and age relationships between the Pelican decollement zone and Sturgeon–Weir Shear Zone. *In* Trans-Hudson Orogen Transect. Report of the 6th Transect Meeting, Saskatoon, Sask., April 1–2, 1996. Lithoprobe Report 55, pp. 73–78.

Ashton, K.E., Hartlaub, R.P., and Lewry, J.F. 1997. The case for a Flin-Flon Glennie protocontinent. Trans-Hudson Orogen Transect. Report of the 7th Transect Meeting, Saskatoon, Sask., May 1–2, 1997. Lithoprobe Report 62, pp. 1–5.

Ashton, K.E., Heaman, L.M., Lewry, J.F., Hartlaub, R.P., and Shi, R. 1999. Age and origin of the Jan Lake Complex; a glimpse at the buried Archean craton of the Trans-Hudson Orogen, Canadian Journal of Earth Sciences, **36**: 185–208.

Baird, D.J., and Clowes, R.M. 1996. Integrating geological, potential field and seismic data in the western Trans-Hudson Orogen. *In* Trans-Hudson Orogen transect. Report of the 6th Transect Meeting, Saskatoon, Sask., April 1–2, 1996. Lithoprobe Report 55, pp. 197–207.

Baird, D.J., Nelson, K.D., Knapp, J.H., Walters, J.J., and Brown, L.D. 1996. Crustal structure and evolution of the Trans-Hudson Orogen; results from seismic reflection profiling. Tectonics, **15**: 416–426.

Bank, C.-G., Bostock, M.G., Ellis, R.M., Hajnal, Z., and VanDecar, J.C. 1998. Lithospheric mantle structure beneath the Trans-Hudson Orogen and the origin of diamondiferous kimberlites. Journal of Geophysics Research, **103**: 10 103 – 10 114.

Bezdan, S., and Hajnal, Z. 1996. Coincident vibroseis and dynamite surveys across the western flank of the Trans Hudson Orogen. Tectonophysics, **264**: 101–109.

Boerner, D.E., Kurtz, R.D., and Craven, J.A. 2000. A summary of electromagnetic studies on the Abitibi–Grenville transect. Canadian Journal of Earth Sciences, **37**: 427–437.

Chiarenzelli, J.R., Aspler, L., and Villeneuve, M. 1996. Characterization, origin, and Paleoproterozoic history of the Saskatchewan Craton and possible implications for Trans-Hudson Orogen, *In* Trans-Hudson Orogen Transect. Report of the 3rd Transect Meeting, Regina, Sask., April 1–2, 1993, Lithoprobe Report 34, pp. 26–38.

Clowes, R.M. (*Editor*). 1989. Lithoprobe Phase III Proposal — the evolution of a continent. Lithoprobe Secretariat, The University of British Columbia, Vancouver, B.C.

David, J., Bailes, A.H., and Machado, N. 1996. Evolution of the Snow Lake portion of the Paleoproterozoic Flin-Flon and Kisseynew belts, Trans-Hudson Orogen, Manitoba, Canada. Precambrian Research, **80**: 107–124.

Elliot, C.G. 1996. The Tabbernor Fault in four dimensions, *In* Trans-Hudson Orogen Transect. Report of the 6th Transect Meeting, Saskatoon, Sask., April 1–2, 1996. Lithoprobe Report 55, pp. 5–9.

Fischer, G., Schnegg, P., and Peguiron, M. 1981. An analytic one-dimensional magnetotelluric inversion scheme. Geophysical Journal of the Royal Astronomical Society, **67**: 257–278.

Ferguson, I.J., Jones, A.G., Yu Sheng, Wu, X., and Shiozaki, I. 1999. Geoelectric response and crustal electrical-conductivity structure of the Flin Flon Belt, Trans-Hudson Orogen, Canada. Canadian Journal of Earth Sciences, **36**: 1917–1938.

Ferguson, I.J., Craven, J.A., Kurtz, R.D., Boerner, D.E., Bailey, R.C., Wu, X., Orellana, M.R., Spratt, J., Wennberg, G., and Norton, M. 2005. Geoelectric response of Archean lithosphere in the western Superior Province, Central Canada. Physics of the Earth and Planetary Interiors, **150**: 123–143.

Grant, N.J. 1997*a*. Processing, interpretation and databasing of magnetotelluric data from the Trans-Hudson Orogen: Site-by-site and multi-site, multi-frequency Groom-Bailey decompositions. *In* Trans-Hudson Orogen. Report of the 7th Transect Meeting, Saskatoon, Sask., May 1–2, 1997. Lithoprobe Report 62, pp. 62–105.

Grant, N.J. 1997*b*. Processing, interpretation and databasing of magnetotelluric data from the Trans-Hudson Orogen: Rapid 2D inversion of the THO92 regional datasets: A summary of results and methodology. *In* Trans-Hudson Orogen Transect. Report of

the 7th Transect Meeting, Saskatoon, Sask., May 1–2, 1997. Lithoprobe Report 62, pp. 16–61.

Groom, R.W., and Bailey, R.C. 1989. Decomposition of magnetotelluric impedance tensor in the presence of local three-dimensional galvanic distortion. Journal of Geophysical Research, **94**: 1913–1925.

Groom, R.W., and Bailey, R.C. 1991. Analytical investigations of the effects of near-surface three-dimensional galvanic scatterers on MT tensor decomposition. Geophysics, **56**: 496–518.

Groom, R.W., Kurtz, R.D., Jones, A.G., and Boerner, D.E. 1993. A quantitative method to extract regional magnetotelluric impedances and determine the dimension of the conductivity structure. Geophysical Journal International, **115**: 1095–1118.

Hajnal, Z., Lucas, S., White, D., Lewry, J., Bezdan, S., Stauffer, M.R., and Thomas, M.D. 1996. Seismic reflection images of high-angle faults and linked detachments in the Trans-Hudson Orogen. Tectonophysics, **15**: 427–439.

Hajnal, Z., Németh, B., Clowes, R.M., Ellis, R.M., Spence, G.D., Burianyk, M.J.A., Asudeh, I., White, D.J., and Forsyth, D. 1997. Mantle involvement in lithospheric collision: Seismic evidence from the Trans-Hudson Orogen, western Canada. Geophysical Research Letters, **24**: 2079–2082.

Hajnal, Z., Lewry, J., White, D., Ashton, K., Clowes, R., Stauffer, M., Gyorfi, I., and Takacs, E. 2005. Seismic reflection signatures of the western Trans-Hudson Orogen. Canadian Journal of Earth Sciences, **42**: this issue.

Jones, A.G. 1986. Parkinson's pointers' potential perfidy. Geophysical Journal of the Royal Astronomical Society, **87**: 1215–1224.

Jones, A.G. 1988. Static shift of magnetotelluric data in a sedimentary basin environment. Geophysics, **53**: 967–978.

Jones, A.G. 1992. Electrical conductivity of the lower continental crust. *In* Continental lower crust. *Edited by* D.M. Fountain, R.J. Arculus, and R.W. Kay. Elsevier, Amsterdam, The Netherlands, pp. 81–143.

Jones, F.W., and Correia, A. 1992. Magneto-telluric soundings in the frequency range 0.01–130 Hz in northern Saskatchewan. *In* Lithoprobe Trans-Hudson Orogen Transect. University of saskatchewan, Saskatoon, Sask., March 9–10, 1992. Lithoprobe Report 26, pp. 111–116.

Jones, A.G., and Ferguson, I.J. 2001. The electric Moho. Nature (London), **409**: 331–333.

Jones, A.G., and Jödicke, H. 1984. Magnetotelluric transfer function estimation improvement by a coherence-based rejection technique. *In* Proceedings of 54th Annual International Meeting, Society of Exploration Geophysics, Atlanta, Georgia, USA. pp. 51–55.

Jones, F.W., and Kalvey, A. 1993. Magnetotelluric measurements between 106°–107°W and 55.5°–55.75°N in northern Saskatchewan. *In* Trans-Hudson Orogen Transect. Report of the 3rd Transect MeetingRegina, Sask., April 1–2, 1993. Lithoprobe Report 34, pp. 56–62.

Jones, A.G., Chave, A.D., Egbert, G., Auld, D., and Bahr, K. 1989. A comparison of techniques for Magnetotelluric response function estimation. Journal of Geophysical Research, **94**: 14 201 – 14 213.

Jones, A.G., Craven, J.A., McNeice, G.W., Ferguson, I.J., Boyce, T.T., Farquharson, C., and Ellis, R. 1993. North American Central Plains conductivity anomaly within the Trans-Hudson orogen in northern Saskatchewan, Canada. Geology, **21**: 1027–1030.

Jones, A.G., Katsube, J., and Schwann, P. 1997*a*. The longest conductivity anomaly in the world explained: sulphides in fold hinges causing very high electrical anisotropy. Journal of Geomagnetism and Geoelectricity, **49**: 1619–1629.

Jones, A.G., Garcia, X., Grant, N.J., Ledo, J., and Ferguson, I.J. 1997*b*. Regional electric structure of the Trans-Hudson Orogen. *In* Trans-Hudson Orogen Transect. Report of the 7th Transect Meeting, Saskatoon, Sask., May 1–2, 1997. Lithoprobe Report 62, pp. 130–146.

Jones, A.G., Snyder, D., Hanmer, S., Asudeh, I., White, D., Eaton, D., and Clarke, G. 2002. Magnetotelluric and teleseismic study across the Snowbird Tectonic Zone, Canadian Shield: A Neoarchean mantle suture? Geophysical Research Letters, **29**: doi: 10.1029/2002GL015359.

Jones, A.G., Ledo, J., and Ferguson, I.J. 2005. Electromagnetic images of the Trans-Hudson orogen: The North American Central Plains (NACP) anomaly revealed. Canadian Journal of Earth Sciences, **42**: this issue.

Katsube, T.J., Jones, A.G., Scromeda, N., and Schwann, P. 1996. Electrical characteristics of rock samples from the La Ronge Domain of the Trans-Hudson Orogen, northern Saskatchewan. *In* Current research, part E. Geological Survey of Canada, Paper 96-1E, pp. 159–169.

Lewry, J.F., and Collerson, K.D. 1990. The Trans Hudson Orogen: extent, subdivision, and problems. *In* The Early Proterozoic Trans Hudson Orogen of North America. *Edited by* J.F. Lewry and M.R. Stauffer. Geological Association of Canada, Special Paper 37, pp. 1–14.

Lewry, J.F., Thomas, D.J., Macdonald, R., and Chiarenzelli, J. 1990. Structural relations in accreted terranes of the Trans-Hudson Orogen, Saskatchewan: telescoping in a collisional regime. *In* The Early Proterozoic Trans Hudson Orogen of North America. *Edited by* J.F. Lewry and M.R. Stauffer. Geological Association of Canada Special Paper 37, pp. 75–94.

Lewry, J.F., Hajnal, Z., Green, A., Lucas, S.B., White, D., Stauffer, M.R., Ashton, K.E., Weber, W., and Clowes, R. 1994. Structure of a Paleoproterozoic continent–continent collision zone: a LITHOPROBE seismic reflection profile across the Trans-Hudson Orogen, Canada. Tectonophysics, **232**: 143–160.

Lucas, S.B., White, D., Hajnal, Z., Lewry, J., Green, A., Clowes, R., Zwanzig, H., Ashton, K., Schledewitz, D., Stauffer, M., Norman, A., Williams, P.F., and Spence, G. 1994. Three-dimensional collisional structure of the Trans Hudson Orogen, Canada. Tectonophysics, **232**: 161–178.

Lucas, S.B., Stern, R.A., Syme, E.C., Reilly, B.A., and Thomas, D.J. 1996. Intraoceanic tectonics and the development of continental crust: 1.92–1.84 Ga evolution of the Flin Flon Belt, Canada. Geological Society of America Bulletin, **108**: 602–629.

Lucas, S.B., Hajnal, Z., and Lewry, J.F. 1997. Towards a synthesis of the Trans-Hudson Orogen Transect: highlights from the Phase V proposal. *In* Trans-Hudson Orogen Transect. Lithoprobe Report of the 7th Transect Meeting, Saskatoon, Sask., May 1–2, 1997. Report 62, pp. 227–250.

MacDonald, R., and Broughton, P. 1980. Geological map of Saskatchewan, Provisional edition, Saskatchewan Geological Survey, map scale 1 : 1 000 000.

Maxeiner, R.O., Sibbald, T.I.I., Slimmon, W.L., Heaman, L.M., and Watters, B.R. 1999. Lithogeochemistry of volcanic–plutonic assemblages of the southern Hanson Lake Block and southeastern Glennie Domain, Trans-Hudson Orogen: evidence for a single island arc complex. Canadian Journal of Earth Sciences, **36**: 209–255.

McNeice, G., and Jones, A.G. 2001. Multisite, multifrequency tensor decomposition of magnetotelluric data. Geophysics, **66**: 158–173.

Németh, B., Hajnal, Z., and Lucas, S.B. 1996. Moho signature from wide-angle reflections: preliminary results of the 1993 Trans-Hudson Orogen refraction experiment. Tectonophysics, **264**: 111–121.

Pandit, B.I., Hajnal, Z., Stauffer, M.R., Lewry, J., and Ashton, K.E.

1998. New seismic images of the cross in the central Trans-Hudson orogen of Saskatchewan. Tectonophysics, **290**: 211–219.

Parkinson, W.D. 1962. The influence of continents and oceans on geomagnetic variations. Geophysical Journal of the Royal Astronomical Society, **6**: 441–449.

Rodi, W., and Mackie, R.L. 2001. Nonlinear conjugate gradients algorithm for 2-D magnetotelluric inversion. Geophysics, **66**: 174–187.

Schwerdtner, W.M., and Cote, M.L. 2001. Patterns of pervasive shear strain near the boundaries of the La Ronge Domain, inner Trans-Hudson Orogen, western Canadian Shield. Precambrian Research, **107**: 93–116.

Smith, J.T., and Booker, J.R. 1991. Rapid inversion of two- and three-dimensional magnetotelluric data. Journal of Geophysical Research, **96**: 3905–3922.

Stevens, K.M. 1998. The Interpretation of Magnetotelluric Measurements from the Glennie Domain to the Flin Flon Belt, eastern Saskatchewan: Part of the LITHOPROBE, Trans Hudson Orogen Transect. M.Sc. thesis, University of Manitoba, Winnipeg, Man., Canada.

Symons, D.T.A., Gala, M., and Palmer, H.C. 1995. Fitting paleomagnetic data to a plate tectonic model for the Trans-Hudson Orogen with focus on the Hanson Lake block. *In* Trans-Hudson Orogen Transect. Report of the 4th Transect Meeting, Saskatoon, Sask., April 11–12, 1994. Lithoprobe Report 38, pp. 18–26.

Thomas, M.D., and Tanczyk, E.I. 1993. Gravity, magnetic and rock property studies in support of Trans-Hudson Orogen Transect. *In* Trans Hudson Orogen Transect. Report of the 3rd Transect Meeting, Regina, Sask., April 1–2, 1993. Lithoprobe Report 34, pp. 63–70.

Vozoff, K. 1991. The magnetotelluric method. *In* Electromagnetic methods in applied geophysics — Vol. 2. Applications. *Edited by* M.N. Nabighian. Society of Exploration Geophysicists, Tulsa, Okla., USA., pp. 641–711.

White, D.J., Lucas, S.B., Hajnal, Z., Green, A.G., Lewry, J.F., Weber, W., Bailes, A.H., Syme, E.C., and Ashton, K. 1994. Paleo-Proterozoic thick-skinned tectonics: Lithoprobe seismic reflection results from the eastern Trans Hudson Orogen. Canadian Journal of Earth Sciences, **31**: 458–469.

White, D.J., Jones, A.G., Lucas, S.B., and Hajnal, Z. 1999. Tectonic evolution of the Superior Boundary Zone from coincident seismic reflection and magnetotelluric profiles. Tectonics, **18**: 430–451.

White, D., Boerner, D., Wu, J., Lucas, S., Berrer, E., Hannila, J., and Somerville, R. 2000. Mineral exploration in the Thompson Nickel Belt, Manitoba using seismic and controlled-source EM methods. Geophysics, **65**: 1871–1881.

Yeo, G.M., Ashton, K.E., Delaney, G., Harper, C., and Maxeiner, R.O. 2001. An update on the western Trans-Hudson orogen in Saskatchewan. Geological Association of Canada, Programs and Abstracts, **26**: 166.